Winter 2006

Diverse Effects of Nanosecond Pulsed Electric Fields on Mammalian Cells

Jody Anne White
Old Dominion University

DIVERSE EFFECTS OF NANOSECOND PULSED ELECTRIC FIELDS ON MAMMALIAN CELLS

by

Jody Anne White
B.S. Biology, May 1998, University of North Carolina at Wilmington

A Dissertation Submitted to the Faculty of
Old Dominion University in Partial Fulfillment of the
Requirement for the Degree of

DOCTOR OF PHILOSOPHY

BIOMEDICAL SCIENCES

OLD DOMINION UNIVERSITY
December 2006

Approved by:

Stephen J. Beebe (Director)

Peter F. Blackmore (Member)

Richard Nuccitelli (Member)

Karl H. Schoenbach (Member)

ABSTRACT

DIVERSE EFFECTS OF NANOSECOND PULSED ELECTRIC FIELDS ON MAMMALIAN CELLS

Jody Anne White
Old Dominion University, 2006
Director: Dr. Stephen J. Beebe

The continuing effort to manipulate cell-signaling pathways for therapeutic benefit has lead to the exploration of electric field effects on cells. Current electric field applications include electroporation of the plasma membrane for introduction of drugs, genes, or other macromolecules into cells. Modeling of how these pulsed electric fields affect cells depicts the cell as an excitable circuit. In this model, the electric fields, administered in short pulses to a cell, charge the plasma and internal membranes, which act as dielectric layers, and between these the cytoplasm acts as a conductive medium. The pulse lengths of this treatment are traditionally in the range of 0.1 to 20 ms. Since the pulse duration is longer than the charging time of the plasma membrane the accumulation of charges along the membrane effectively shields the intracellular components from the imposed electric field much like a Faraday cage. With advances in pulsed power technology sub-microsecond pulses are now possible. This timescale is shorter than the charging time of the plasma membrane and therefore, during an applied field of sufficiently short duration and higher potential, charges are unable to accumulate sufficiently around the plasma membrane. This allows the applied field to be experienced throughout the interior of the cell. Thus it is proposed that pulsed electric fields of ultra short duration (<1 μs) may manipulate specific intracellular functions. Based on molecular modeling of nanosecond duration pulsed electric fields (nsPEFs) the short duration of the pulse does not contribute to significant electroporation in the conventional sense. Rather a large number of nano-pores are formed, or supra-electroporation, that can limit large molecules from intracellular entry but may allow non-specific ion traffic. Therefore, nsPEFs are hypothesized to affect intracellular membrane structures providing a new means to modulate signal transduction mechanisms. This study investigated the effects of nsPEFs on induced calcium mobilization and changes in transmembrane potential in cultured cells. The results may further the development of nsPEFs as a basic investigative tool for discovery of new signaling pathways and stimulation of cell function. This application also holds promise as a possible medical treatment for tumor reduction and platelet activation.

This dissertation is dedicated to my grandparents who always encouraged my curiosity and goals in academics.

ACKNOWLEDGMENTS

I would like to express gratitude to my family and friends who encouraged my academic pursuits. For the members of my research committee I would like to extend many thanks for their ideas, support, and the example they set for me as committed researchers.

TABLE OF CONTENTS

LIST OF FIGURES

Figure Page

Figure Page

CHAPTER I

INTRODUCTION

In the arena of biomedical research a large proportion of work is focused on alleviating human physical maladies or enhancing physical function. The human body relies on the interaction of a number of systems to enact movement, respiration, nutrient processing, homeostasis, and cognitive abilities. Although these systems are very different, when broken down to their constituent parts, they are based on a single core piece, the mammalian cell. Each cell contained in tissue, nerves, muscle, skin, etc. has a similar make-up in that it contains most of the same organelles and has more or less the same construction, a plasma membrane surrounding an amount of cytoplasm and a nucleus. It is each cell's ability to respond to varying stimuli in very different ways that allows an entire system to function uniquely. The study of mammalian cell function has lead most research into defining how a cell is able to respond to these stimuli, or its response pathways termed signal transduction mechanisms. Signaling pathways and networks provide cells the means to respond precisely and effectively to whatever stimulation is encountered within their physiological environment. To understand cell function and processing completely, it is necessary to define these pathways and their interpretations. Traditional tools used to study signaling include the use of introduced proteins or DNA, radiation, and pharmacological agents. These tools provide researchers a means to stimulate cells to perform specific functions or to generate certain products. Although these means have been successful, many conventional stimulants generate undesirable side effects or byproducts that further complicate a study. Studies using electricity as a stimulus are not new to research but due to the interdisciplinary understanding of both biology and engineering principles the field has taken far longer to grow in interest to the scientific community. The use of applied electric fields of relatively short duration on the order of milliseconds to initiate a cell response became popular when it was found that these fields could be used to introduce membrane impermeant molecules into the cell without the use of other stimuli and that it could be done without compromising cell viability. These short applied fields or pulses, described as electroporative, are now quite frequently used to temporarily interrupt membrane integrity. Recent advances in pulsed power technology now allow the development of significantly higher power electric field applications. These high power, low energy fields can be delivered in ultra fast pulses that do not cause significant thermal heating. Ultra-fast, high electric field pulses

---

The model for this dissertation is the *Journal of Biological Chemistry.*

are termed nanosecond pulsed electric fields (nsPEFs) and are hypothesized to affect intracellular structures in living cells by creating an electric field on a time scale faster than the charging time of the plasma membrane. Thus the entire applied field is felt by internal membranes in addition to the plasma membrane providing a new method to modulate cell signal transduction mechanisms. The studies provided herein thus show that access to intracellular areas can be achieved without the unwanted side effects or byproducts normally encountered with the use of traditional stimulants. In other words pulsed electric fields present a new way to stimulate cell function in a more precise manner, inside and out.

Applied Electric Field Model—A model of a cell as an electrical system aids in describing the effects of pulsed electric fields on a cell. The plasma membrane can be depicted as a dielectric layer or capacitor that contains a volume of cytoplasm acting as a conductive medium with measurable resistance (1, 2). When such cells are suspended in a conductive buffer and then treated with pulsed electric fields, generated by placing the cell suspension between two electrodes, charging of the dielectric layers, i.e. the plasma membrane occurs similar to the charging of an ideal capacitor (3). The voltage difference across the plasma membrane that is created by this treatment may exceed a critical value at which membrane poration develops (4). This breakdown in the cell's membrane integrity can occur in two ways. Classical electroporation is the formation of relatively large pores in the plasma membrane with little or no poration of subcellular membranes. These pores may exist only temporarily if the duration and magnitude of the electric field applied remains below a threshold for cell viability (5). Under certain conditions the presence of reversible pores does not compromise cell viability and the plasma membrane eventually regains integrity within minutes (6). The extent to which these electric fields affect the plasma membrane is determined by the cell diameter (D), the resistivity of the cell cytoplasm (ρ_c) and the buffer in which the cells are treated (ρ_a), and the capacitance of the surface membrane per unit area (c_m). The time required to induce plasma membrane breakdown is described as the charging time constant (τ_c), which is equal to [$\tau_c = (\rho_c+\rho_a/2)\cdot c_m D/2$] (7). Although initially pulsed electric field effects were limited to the plasma membrane because pulse lengths were no shorter than microseconds it is now theorized that with ultra-short nanosecond pulses of high electric fields (kV/cm) not only is the plasma membrane porated but also the charging of organelle membranes can occur. This effect was recently termed supra-electroporation and is distinct from conventional electroporation in that only relatively small pores develop in both the plasma and intracellular membranes. These small pores exclude membrane integrity indicators such as propidium iodide and ethidium homodimer that are generally taken into the cell when exposed to electroporation pulses. This process of supra-electroporation allows the electric field to be focused into

internal areas without causing irreversible damage to the plasma membrane. This type of electric field application is promising an unprecedented manipulation of cellular activity (8).

Electroporation History—Starting in the 1980s applied electric fields have been used to introduce xenomolecules into cells (9, 10, 11). The insertion of DNA, viral particles, and other molecules by application of square-wave (12) pulsed electric fields has grown rapidly over the past two decades (5, 13) and is now considered a standard procedure for medicinal and scientific applications. The traditional electroporation procedure usually consists of a low voltage electric field (V-kV/cm) applied in pulses of a few milliseconds to cause the opening of pores in the plasma membrane that allows non-specific entry of molecules of choice either through diffusion or an electrochemical gradient (14, 15, 16). The use of electroporation to introduce chemotherapeutic agents or DNA into cells relies on the pulsed electric field's alteration of the plasma membrane (4, 5, 9). The success of these applications is dependent on cell type and size and the conductivity and composition of the electroporation media (17, 18, 19).

Nanosecond Pulsed Electric Fields history—In the recent decade, advances in pulsed-power technology have allowed the development of pulsers that offer significantly shorter pulse lengths and greater applied voltages in the range of tens to hundreds of kilovolts per centimeter (1, 8, 19, 20). These unipolar pulses are also novel in that the rise time is 1-2 ns, which allows a high voltage square wave pulse (1) to be applied in nanoseconds, which prevents thermal buildup (21, 22). These new apparatuses offer pulse lengths of 10, 60, and 300 ns which when used below threshold electric fields are typically not of sufficient duration to charge the plasma membrane and cause traditional electroporation as witnessed by lack of entry of fluorescent indicator molecules for membrane integrity (21, 22). The proposed focus of these higher power pulses is on internal membranes such as the endoplasmic reticulum and mitochondrial and nuclear membranes (23). This is supported by modeling, as depicted in Fig. 1, which suggests as pulse lengths shorten and electric fields rise the plasma membrane is bypassed in favor of effecting internal structures (21, 22). The most documented effect of these new applied pulses is the stimulation of apoptosis (21, 22). Apoptosis is a pathway in which cells degrade their DNA and other cellular proteins and then target themselves for phagocytosis and thus death (24, 25). Evidence of apoptosis comes from morphological changes in the membranes of the cell and the release of certain caspase proteins and cytochrome c that are indicative of this process occurring (21, 22). These effects are desirable in those studies aimed at development of a cell-specific eradication method. However, at lower kilovolt electric fields of the same nanosecond duration several other exciting effects are seen. Below a threshold electric field that induces apoptotic behavior exists a stimulatory environment in which stimulation of cell signaling and function has been observed. This area

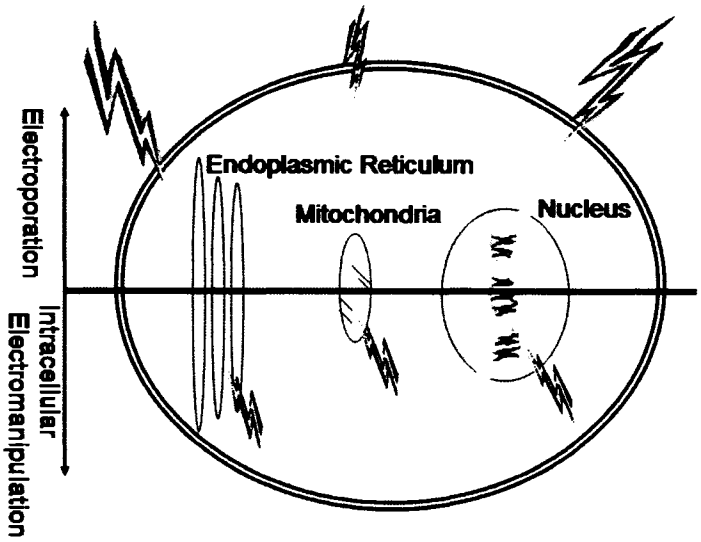

FIG. 1. **Heterogeneity of effects due to nsPEFs.** The combination of pulse duration and electric field applied establishes a threshold where either plasma or intracellular membranes are stimulated.

of research into nsPEFs is growing rapidly because of its wide application to almost all cell types *in vitro* and *in vivo*. In this study, the main focus is on the effect of nsPEFs on 1) intracellular calcium signaling and on 2) changes in transmembrane potentials.

nsPEF Applications—Although nsPEFs are able to cause intracellular electromanipulation as evidenced by apoptosis induction, the mechanism of this stimulation is not understood (21, 22). Electrical theory suggests that these nsPEFs induce pore formation in intracellular membranes similar to electroporation of the plasma membrane (26). This would allow diffusion of key activator molecules or cell signaling ions that may initiate progression through several pathways. Other theories for how nsPEF affects cell signaling as depicted in Fig. 2 include 1) alteration of channel proteins to activate influx of signaling ions, 2) conformational changes in ligand binding sites that mimic natural stimulation and thus activate signaling cascades, and 3) change in the polarization of internal membranes that trigger specific signal transduction mechanisms.

Uniqueness of Stimulation—Currently the forefront of pulsed electric field technology allows for 10, 60, or 300 ns duration pulses at electric field strengths of 4-300 kV/cm. In this study a threshold electric field will be determined for changes in calcium signaling and transmembrane potential. Previously published studies have shown that the 300 and 60 ns pulses above 60 kV/cm typically cause electroporation in Jurkat and HL-60 cells. The studies described herein will de-

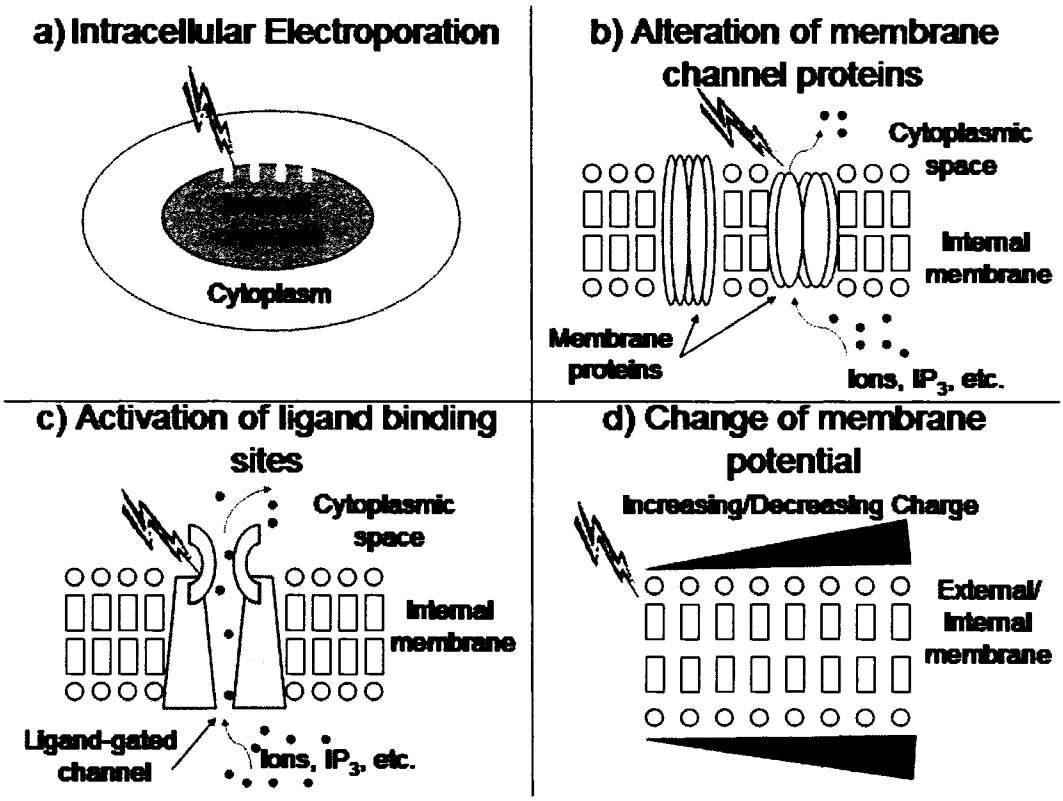

FIG. 2. **Current theories for nsPEF effects.** Extension of electrical modeling of a cell proposes a) electroporation of internal membranes when treated with nsPEF. However, other theories include b) alteration of channel proteins that would allow diffusion of signaling molecules, c) activation of ligand binding sites that mimics natural interactions *in vivo* and d) an increase or decrease in charge buildup at membranes that may also stimulate signaling pathways.

pend solely on the 60 ns pulse duration for stimulation and electric field strengths that include the electroporation range and below. The effects of nsPEF will be compared if possible to traditional agonists that evoke similar responses in our chosen cell models. The use of nsPEFs are unique to traditional stimulations by radiation, drugs, and environmental changes in that the pulses do not leave a residual stimulation in the cell once the treatment ends. There is also no accumulation of stimulus associated with an electric field treatment removing typical concerns of toxicity and thermal effects.

REVIEW OF RESEARCH

Previous work in this area has shown that nsPEFs can induce apoptosis in several cell types including HL-60 and Jurkat cells and can also cause a reduction in fibrosarcoma and B16

melanoma tumor size in mice (21, 22, 27, 28). Apoptosis was defined by evidence of caspase activity, Annexin V binding, DNA degradation, a lack of Propidium Iodide and/or Ethidium Homodimer-1 uptake, and cytochrome c release (21, 22, 27). A threshold applied electric field for apoptosis induction was therefore defined for the above mentioned cell types. Below this apoptosis threshold, cultured cells continue to live and divide. Furthermore they show evidence of enhanced function, cell signaling, and second messenger stimulation.

OVERVIEW OF STUDY

The studies presented here are designed to achieve three major objectives. First, the data will add to increasing evidence that human cells show a heterogeneous response to different applied nsPEFs, which is consistent with the theory for specificity in effects. Second, this work will further the use of applied electric fields for activation of cell function rather than just cell demise and electroporation. Lastly it will help develop a mechanistic view of how these applied electric fields are activating treated cell(s).

Previous studies showed that nsPEF treatment increased apoptosis signaling mechanisms in both Jurkat and HL-60 cells through assays for caspase activation, annexin binding, and cytochrome *c* localization (21, 22). Other preliminary studies using electric fields weaker than those that induce apoptosis have shown to cause a proliferative effect on cells (J.A. White unpublished observations). Therefore, with these pulses it may be possible, depending on the duration and intensity of the electric field applied, to induce varied cell signaling mechanisms resulting in non-apoptotic cellular responses in the same cell type.

Calcium Signaling—In order to enact a response to nsPEF treatment the cell may use physical and/or chemical signals, such as second messengers, to initiate signal transduction cascades within the cell. As seen in Fig. 3 the cell is sensitive to many types of stimuli be it chemical, physical, electrical, etc. and is able to respond uniquely to each type of stimulation by using an assortment of response mechanisms. Calcium signaling is ubiquitous in all cell types and plays a key role in myriad cellular events (29). The well-studied inositol 1, 4, 5-triphosphate (IP_3) pathway as detailed in Fig. 4 involves binding of a ligand to the plasma membrane surface that generates secondary signaling molecules diacylglycerol (DAG) and IP_3. The IP_3 molecules then release IP_3 sensitive calcium stores in the endoplasmic reticulum. The calcium that is released stimulates an influx of calcium from the extracellular medium to amplify the signal and replenish depleted internal stores. Since many cellular functions are dependent on calcium signaling pathways such as the IP_3 pathway to achieve an effect, the response of internal calcium levels to nsPEF stimulation was examined.

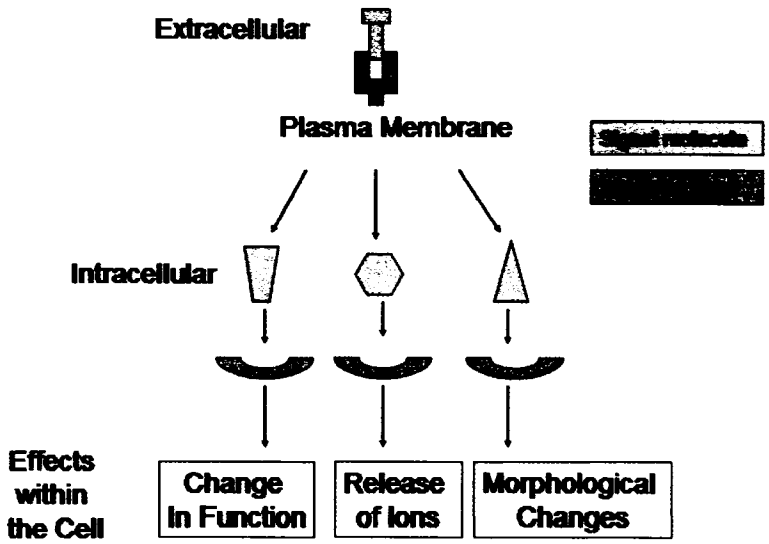

FIG. 3. **Signal transduction in cells uses extracellular and intracellular receptors and signaling molecules in order to transmit response messages that are intracellular and intercellular in nature.** The signaling pathways allow a cell a highly specific and finely tuned means to react to stimulation.

Membrane Potential—In order to fully understand how nsPEF treatment affects cells it is important to determine the initial response to the stimulation. Activation of apoptosis has been initiated by these nsPEFs however this may not be the initial response of the cell. The resting membrane potential(s) of external and internal membranes may be the first parameter that changes in response to nsPEF treatment. In homeostasis cells maintain a negative potential within their plasma membrane (~ 55 – 90 mV depending on cell type) and mitochondrial membrane (~ 150 – 300 mV) in comparison to the external environment. Cells rely on this maintained negative potential to keep normal cellular function. Any change in membrane potential may be interpreted by the cell as a signaling event. Excitable cells have voltage gated ion channels that are sensitive to these changes for their activity. The distribution of ions within and outside the cell give rise to the membrane potential. Different concentrations of potassium, sodium, calcium, etc. are found in compartments within the cell, such as the endoplasmic reticulum, nucleus, and mito chondria. The largest differences in the ion concentrations can be found on either side of the plasma membrane and the mitochondrial membranes. These two membranes represent the largest potentials in the cell. Because ion charges are responsible for the existence of the membrane potentials and because charge distribution can be changed very quickly, especially in the presence of a polarizing electric field, the plasma membrane of Jurkat cells was monitored for changes in

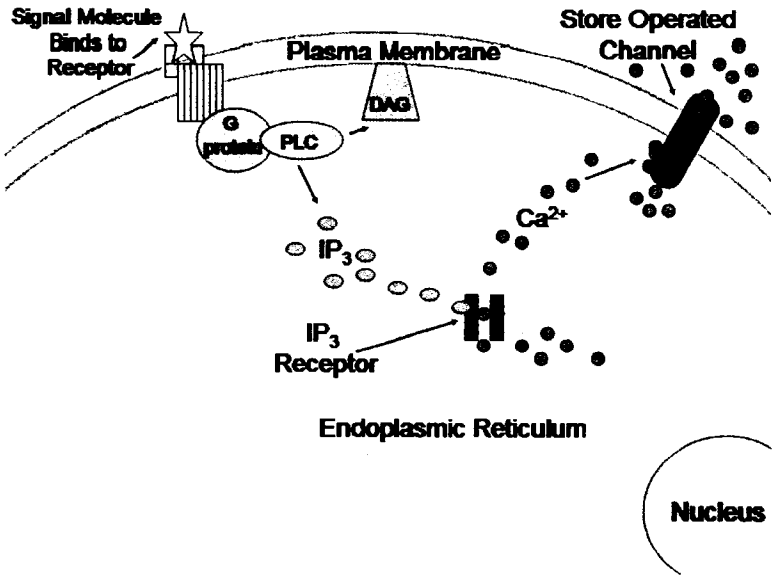

FIG. 4. **Binding of signal molecules to the G-protein linked receptor activates the G protein and subsequently Phospholipase C (PLC).** Activation of PLC produces IP_3 and DAG signaling molecules by hydrolysis of phosphatidylinositol 4, 5-bisphosphate (PIP_2). The IP_3 activates IP_3-receptors in the endoplasmic reticulum releasing stored calcium. The resulting increase in cytoplasmic calcium activates store operated channels in the plasma membrane allowing calcium influx from the extracellular media into the cell to intensify signal transduction and to replenish depleted stores of calcium.

membrane potential due to nsPEF stimulation. Because these changes in ion distribution can occur on a sub-physiological timescale it is possible that this change is the initial response of the cells to nsPEFs. It is postulated that the change in transmembrane potential may trigger other internal signaling events that can be measured in a physiological timescale after nsPEF stimulation. These events include changes in intracellular calcium and changes in membrane conductivity measured on a millisecond timescale. Molecular dynamics modeling supports both the sub-physiological changes in potential and the slower physiological changes. Therefore, in order to establish a complete response pathway of a cell to nsPEFs the initial response needs to be established.

Significance of Study—The results presented here will broaden the scope of how applied electric fields can be used for further exploration of cell biology and how their use may incur health benefits. As an alternative means to stimulate cells, the effects of a pulsed electric field study can be compared to those studies using traditional agonists or other pharmacological means.

This will allow comparison of signaling and response pathways and may allow for discovery of new pathways. In this way, applied electric fields can be developed as a tool for discovery and illumination of signaling pathways. Previous studies have reported that the use of applied electric fields on cancer cells in culture has lead to an increase in caspase activation and subsequently apoptosis (21, 22). As a new therapeutic regimen for external cancers, applied electric fields may provide a chemically-free treatment for malignancies that is specific rather than using a systemic treatment. Published observations of sub-apoptotic effects also support stimulation of cell function and activation. For these reasons the development of applied electric fields for application to mammalian cells is warranted. The uniqueness of nsPEF studies should not only provide insight into cell function and the mechanisms and pathways that bring about the observed effects but also promises to become a therapeutic treatment for cell-specific eradication of diseased or unwanted tissues. Cooperation between basic scientists, engineers, and medical personnel will ensure the development of applied nsPEF to be used in many scientific research areas.

CHAPTER II

STIMULATION OF CAPACITATIVE CALCIUM ENTRY IN HL-60 CELLS BY NANOSECOND PULSED ELECTRIC FIELDS

INTRODUCTION

The release of internally stored calcium in mammalian cells can stimulate responses to agonists, activate growth, and initiate release of key factors in the apoptosis pathway (30). This calcium mobilization also triggers the influx of calcium from the external medium into the cell as a means of further propagating calcium signals and to replenish depleted pools of calcium and is termed capacitative calcium entry. The continuing effort to manipulate cell signaling pathways for therapeutic benefit has led to the exploration of electric field effects on cells (31-34). Current electric field applications include electroporation of the plasma membrane for introduction of drugs, genes, or other macromolecules into cells (11, 35-40). The pulse lengths for this kind of electric field treatment are in the range of 0.1 to 20 ms (34). With advances in pulsed power technology, it has been proposed that pulsed electric fields of ultrashort duration (<1 μs) may manipulate specific intracellular functions (8, 27). Current modeling of how these pulsed electric fields affect cells depict a cell as an excitable circuit (1). In this model, the electric fields administered to a cell charge the plasma and internal membranes, which act as dielectric layers, and between these the cytoplasm acts as a conductive medium. With these ultrashort pulses the plasma membrane is not exposed to an electric field of sufficient duration to charge it to such a voltage that significant electroporation occurs (1). Based on molecular modeling of nanosecond duration pulsed electric fields (nsPEFs) the effects seen should be largely targeted on internal organelle membranes. To study calcium signaling, applied electric fields could be used to manipulate the movement of ions, such as calcium, by interaction with intracellular membranes. Therefore, because of the increasing interest in electric field effects on biological systems, nsPEFs were used to provoke calcium mobilization in mammalian cells.

Previous studies showed that nsPEF treatment increased apoptosis signaling mechanisms in both Jurkat and HL-60 cells through assays for caspase activation, annexin binding, and cytochrome *c* localization (21). Other studies using electric fields weaker than those that induce apoptosis have been shown to cause a proliferative effect on cells. Therefore, with these pulses it may be possible, depending on the duration and intensity of the electric field applied, to induce varied cell signaling mechanisms resulting in non apoptotic cellular responses in the same cell type.

In order to enact such responses to nsPEF treatment, the cell may use physical and/or chemical signals to initiate signal transduction cascades within the cell. Calcium signaling is ubiquitous in all cell types and plays a key role in several cellular events (29). Because many cellular functions are dependent on calcium signaling to achieve an effect, the response of internal calcium levels to nsPEF stimulation was examined.

To compare nsPEF-induced effects on intracellular free calcium ($[Ca^{2+}]_i$), we used the purinergic agonist uridine triphosphate (UTP) (41-44), which has been shown previously to induce calcium fluxes and capacitative calcium entry in HL-60 cells. These agonists induce calcium signaling by binding to a specific purinergic receptor of the $P2Y_2$ (previously called P_{2U}) subtype (41, 42). $P2Y_2$ receptors were shown previously to be present in HL-60 cells (45). This receptor signaling involves G protein activation of phospholipase C (PLC) with a subsequent increase in the second messenger inositol 1,4,5-trisphosphate (IP_3) (for review see Ref. 29). IP_3 then initiates the release of calcium from IP_3-sensitive calcium stores into the cytoplasm. This increase in calcium stimulates the opening of store-operated channels in the plasma membrane allowing influx of calcium into the cell for replenishment of the internal stores. This influx is believed to be via a capacitative calcium entry (CCE) mechanism. The precise molecular nature of the CCE pathway in many cells is unknown. However, there is much evidence suggesting that members of the transient receptor potential (TRP) family of proteins may act as the plasma membrane calcium channel. The TRP proteins are classified as TRPC (canonical), TRPV (vanilloid), and TRPM (melastatin) (46). The transmembrane architecture of the TRPs is similar to voltage-gated and cyclic nucleotide-gated channels. HL-60 cells are positive for TRPC1, TRPC2, TRPC3, TRPV1, TRPV2, TRPV5, TRPV6, and TRPM2 (47). From this collection of channel proteins, TRPC1, TRPC3, TRPC4, and TRPV6 have been shown to participate in CCE (48). Therefore, HL-60 cells possess several candidates that could act as CCE channels.

How the internal calcium store depletion communicates to the CCE process in the plasma membrane is still being studied. Two main theories exist for this coupling as follows: the first suggests physical interaction between the IP_3 receptor in the ER and the CCE channel, and the second suggests the existence of a secondary messenger molecule or calcium-inducing factor (49, 50).

Preliminary reports showing that nsPEF stimulation of HL-60 cells increased $[Ca^{2+}]_i$ were presented at ElectroMed (22) and SPRBM (51) conferences. The purpose of this study was to investigate the mechanism by which nsPEF increased $[Ca^{2+}]_i$. The data show that nsPEF can induce calcium transients similar to those seen following purinergic receptor stimulation and thapsigargin. This response was observed in the absence of classical plasma membrane electropora-

tion. Previous studies in HeLa cells showed that classical electroporation pulses (100 μs, 500 V/cm) also stimulated calcium responses similar to those seen with hormones (52). The results presented here further support the hypothesis that when nsPEFs that are below the threshold for plasma membrane electroporation and apoptosis induction are applied, intracellular signal transduction cascades can be triggered, resulting in signaling events that are common with natural ligands. The application of nsPEFs to cells and tissues provides a new tool to investigate signal transduction mechanisms, including calcium signaling, by modulating intracellular release, and capacitative calcium entry through receptors in the plasma membrane.

EXPERIMENTAL PROCEDURES

Cell Culture—Non-transformed HL-60 cells were used for this study and were obtained from American Type Culture Collection (ATCC, Manassas, VA). They were cultured in 75 cm^2 flasks in phenol red RPMI 1640 medium (Mediatech Cellgro) supplemented with 20% fetal bovine serum (Atlanta Biologicals, Norcross, GA), 1% L-glutamine, and 1% penicillin/streptomycin (Mediatech Cellgro) and incubated at 37 °C with 5% CO_2. HL-60 cells in log-phase were removed from the culture and resuspended in a physiological buffer containing 145 mM NaCl, 5 mM KCl, 0.4 mM NaH_2PO_4, 1 mM $MgSO_4 \cdot 7H_2O$, 6 mM glucose, 5 mM HEPES (pH 7.4) prior to experimentation. 1.5 mM $CaCl_2$ was added to this buffer when loading cells with fluorescent indicators unless otherwise stated. In some experiments extracellular calcium was omitted by washing the cells at least once in the same physiological buffer without added calcium. The addition of 1.5 mM EGTA prior to nsPEF treatment in a few of the initial experiments ensured that the small amount of calcium that was present in the calcium-deficient buffer was chelated. Total calcium in the buffer was measured by atomic absorption spectroscopy and was found to be 1.5 ± 0.05 mM in the presence of calcium and 3.06 ± 0.35 μM in buffer without added calcium (n = 3).

Administration of nsPEF—Cell suspension (7.7 x 10^6 cells/ml) was added into the Bio Rad gene pulser cuvettes prior to nsPEF treatment. nsPEF was delivered by means of a cable pulse generator to a cuvette with two parallel plate electrodes, separated by 0.4 cm, containing cell suspensions. The electric fields administered were 4, 6.5, 10, and 15 kV/cm. The generator consisted of a 10 ohm pulse-forming network (five 50 ohm cables in parallel) and a spark gap in atmospheric air as a nanosecond closing switch (21). Post pulse, the cell suspension was removed from the nsPEF cuvette and assayed. Cell viability was ≥95% indicating that these nsPEF conditions were below the threshold for apoptosis or necrosis.

Microscopic Analysis of Internal Calcium Response—An Olympus photomicroscope with a Kodak DC-120 digital camera was used with the fluorescent indicator Fluo-3, AM (Molecular

Probes, Eugene, OR) to assess changes in intracellular free calcium. HL-60 cells were suspended in the above-described physiological buffer containing 2 mM calcium. Fluo-3, AM (2 μM) was added to the cells, and the cells were then incubated at 37 °C for 45 min. The cells were then washed and resuspended in the physiological buffer with or without 2 mM calcium. An aliquot of HL-60 cell suspension was loaded into a space between metal electrodes affixed to a slide for real time monitoring of calcium transients. A description of this nsPEF apparatus can be found in the article by Deng *et al.* (53). To analyze the cell response, Merlin software (PerkinElmer Life Sciences) was used to detect changes in gray scale of the selected cell areas, and we compared these changes to a background region.

Assessment of Membrane Integrity—Propidium iodide (PI) (Molecular Probes, Eugene, OR), at a final concentration of 10 μg/ml, was added to HL-60 cell suspension (7.7 x 10^6 cells/ml) in a 0.4 cm BioSmith cuvette. For each of the four electric field settings, the cells were given one 60 ns pulses. Immediately following nsPEF stimulation, the cells were then removed from the cuvettes and transferred to flow cytometry vials for analysis (CellQuest software) on a FACSCalibur flow cytometer (BD Biosciences). As a positive control, 0.1% Triton was added to the cells to induce membrane disruption in the presence of PI. The cell suspensions were analyzed within 2 min of treatment.

Fluorometric Analysis of Internal Calcium Response—To analyze the response of a greater number of cells, the fluorescent indicator Fura-2, AM (Molecular Probes, Eugene, OR) was used with a fluorometer. HL-60 cells were incubated with Fura-2, AM (2 μM) in the physiological buffer described above containing 2 mM calcium for 45 min at 37 °C. The cells were then washed and resuspended in calcium-free or calcium-containing buffer at a concentration of 7.7 x 10^6 cells/ml. Calcium measurements were performed in a SPEX ARCM spectrofluorometer, similar to that described previously (54). HL-60 cells were first placed in the fluorometer cuvette, to obtain a base-line reading, and cells were then removed from the fluorometer cuvette with a Pasteur pipette and added to the BioSmith cuvette. Cells were treated with nsPEF (8) and then immediately removed from the BioSmith cuvette and added back to the fluorometer cuvette (located in close proximity to the pulse generator, which took between 5 and 10 s), and the fluorescence measurements were continued. For those experiments that included the addition of UTP, an aliquot of UTP was pipetted into the BioSmith cuvette and mixed by pipetting up and down gently. For Fig. 7, *A* and *B*, BioSmith electroporation cuvettes were used to perform calcium measurements in the fluorometer by using a fiber optic light guide. The cells were excited at 340 and 380 nm through the clear side of the cuvette between the aluminum plates. The light emitted from the top of the cuvette was transmitted to the photomultiplier by using a fiber optic light guide. HL-60

cells were placed in the cuvette to which 1.5 mM EGTA was added and mixed into the cell suspension, and a base-line fluorescence reading was acquired. The cuvette was then removed from the fluorometer and treated with nsPEF (8) and then immediately replaced into the fluorometer (located in close proximity to the pulse generator, which took between 5 and 10 s), and the fluorescence measurements were continued. Although this method produced reliable results, the fluorescence signals contained noise. This was reduced significantly by removing the cell suspension from the BioSmith cuvette after treatment and transferring it to the fluorometer cuvette. Figs. 5 and 8-12 were prepared by using this method.

RESULTS

Single Cell Analysis of the Effect of nsPEF on Intracellular Free Calcium—In order to assess how nsPEF stimulation affects internal events in cells, real time microscopic analysis of cells with the fluorescent calcium indicator Fluo-3 was utilized. HL-60 cell suspension was loaded into the nsPEF slide (53), and a group of cells in the field of vision between the electrodes was chosen to analyze. Typically 10–15 cells could be viewed at one time, and their response to nsPEF was recorded. All cells that were present in the field of view of the microscope were analyzed for changes in internal calcium. In Fig. 5, each cell in the field of view of the microscope is represented as an individual line, and the average response was presented as a heavy line. The fluorescence of each cell was monitored over the time of the experiment and was compared with background. Following the nsPEF pulse (Fig. 5, black arrow), all of the cells responded with an increase in $[Ca^{2+}]_i$. This coordinated increase in $[Ca^{2+}]_i$ was not seen in untreated cells. This increase in $[Ca^{2+}]_i$ following nsPEF could result from intracellular calcium mobilization followed by CCE.

nsPEF Does Not Induce Electroporation of the Plasma Membrane at Low Electric Fields—From Fig. 5 a rise in intracellular calcium is seen when cells are treated with nsPEF. The next step was to determine whether this increase was because of influx from the extracellular media or from internal store release. Our hypothesis states that nsPEF should affect internal membranes; therefore, the increase in $[Ca^{2+}]_i$ because of nsPEF stimulation would result from internal store release. To test this theory, evidence of plasma membrane electroporation at the electric fields used in this study was investigated. Classical electroporation experiments applied electric fields of sufficient duration to induce dielectric breakdown in the plasma membrane (13, 55). To assess plasma membrane integrity under our experimental conditions, the indicator PI was used with flow cytometry. The data revealed no increase in PI uptake when compared with control (control averaged 1.5 ± 0.5% and the highest electric field used for treatment averaged 0.9 ± 0.3%

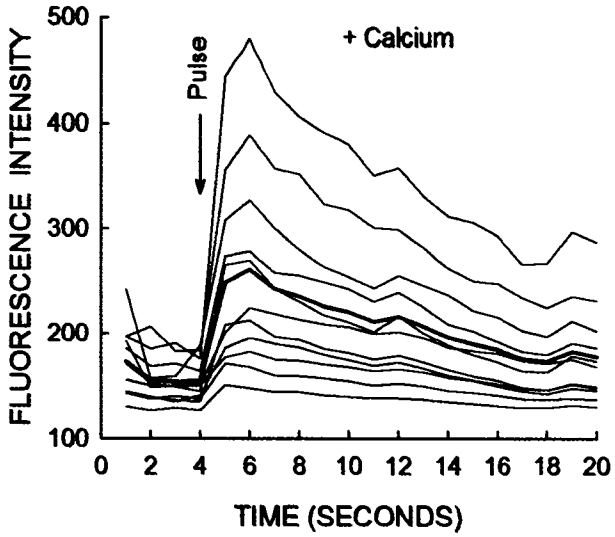

FIG. 5. **HL-60 cells respond to nsPEF treatment by increasing intracellular calcium.** HL-60 cells, loaded with Fluo-3, AM fluorescent indicator in the presence of extracellular calcium, were stimulated with one 60 ns pulse (30 kV/cm) and analyzed in real time. Images were taken as frames at 10 s intervals. Where an nsPEF pulse was administered, the majority of cells showed an increase in fluorescence compared with base line (*p* value 0.004). The average response of 22 untreated cells is shown as a *dashed line* with *error bars* representing S.E. Data are representative of three separate experiments.

fluorescence gated for PI). In all subsequent experiments in this study, cells were treated within this electric field range to ensure plasma membrane integrity.

Effect of UTP on HL-60 Cells in the Presence and Absence of Extracellular Calcium— Because evidence of plasma membrane electroporation was not found, the increase in $[Ca^{2+}]_i$ due to nsPEF stimulation, in the absence of extracellular calcium, is likely to be coming from the release of internal stores. A traditional agonist, UTP, which induces internal store release, was used as a stimulus, and the response of the cell was compared with the response to nsPEF. Fig. 6 shows a representative experiment of HL-60 cells that were treated with 10 μM UTP in the presence of 1.5 mM calcium and in the absence of calcium, by chelation with 1.5 mM EGTA. If an increase in calcium is seen in the absence of extracellular calcium, then the source of the increase must be internal stores. The 1.5 mM EGTA, however, caused an unexpected response of "drain-

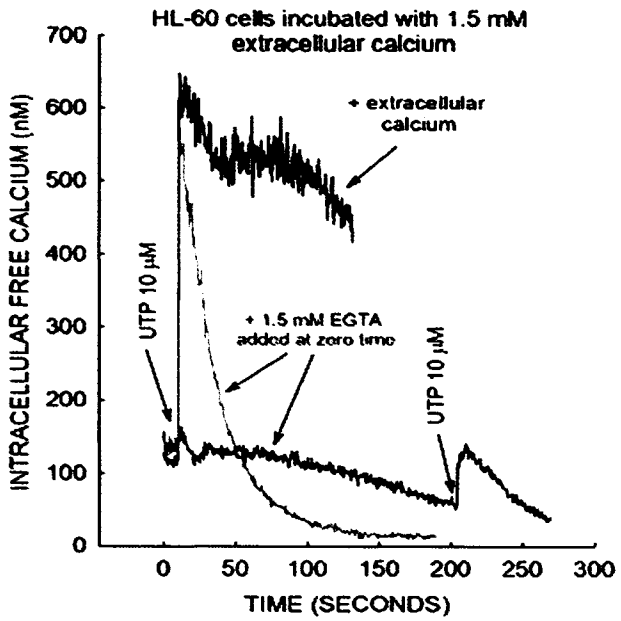

FIG. 6. **HL-60 cells, stimulated by nsPEF, respond by releasing internal calcium stores.** HL-60 cells incubated with extracellular calcium (1.5 mM) respond to nsPEF with a substantial and relatively prolonged release of $[Ca^{2+}]_i$. Cells incubated in calcium-deficient media with added 1.5 mM EGTA respond with similar magnitude; however, the response is quite transient (*gray trace*). This response represents release of internal stores of calcium. HL-60 cells incubated in the same calcium-deficient conditions were allowed to lose some of their calcium before treating with UTP. The gradual loss of calcium before treatment strongly suggests that calcium influx through the plasma membrane is not occurring and that the response seen to UTP is because of internal store release.

ing" the cell of internal calcium. When EGTA was added to HL-60 cell suspension, the calcium concentration, as measured with Fura-2, began to decrease shortly after addition as seen in Fig. 6. This is because of the EGTA chelating the extracellular calcium and then creating an unfavorable calcium sink that causes the cell to extrude its internal calcium stores into the extracellular media. Therefore, HL-60 cells are unable to maintain their internal calcium stores for very long (~100 s) when placed in a calcium-deficient environment. A dose-response experiment of EGTA (1.0, 1.5, 2.0, and 3.0 mM) to HL-60 cells allowed us to choose an amount of EGTA that chelates most of

the extracellular calcium but does not cause a draining of internal stores as rapidly as higher concentrations (data not shown). In order to create an environment void of extracellular calcium and still see an increase in calcium because of the addition of UTP or nsPEF, the stimulus had to be given quickly after the EGTA-induced calcium decrease was seen. The initial increase in calcium to UTP in the absence of calcium (presence of EGTA) was similar to that seen in the presence of extracellular calcium; however, the response was considerably more transient. The $[Ca^{2+}]_i$ decreased to basal values at 50 s and to ~10 nM after 150 s when extracellular calcium was low. According to our measurements, the concentration of extracellular calcium in the calcium-deficient media was 3 μM; therefore, in an environment where there exists a gradient of calcium, higher in the extracellular calcium, calcium entry into the cell was still not occurring after stimulation, rather efflux was evident. In Fig. 6 HL-60 cells were incubated with 1.5 mM EGTA until the $[Ca^{2+}]_i$ began to fall below basal levels, such that by 200 s the $[Ca^{2+}]_i$ was ~50% of that seen at zero time. The cells then were stimulated with 10 μM UTP at 200 s, and a modest yet transient response of about 50 nM was still seen, confirming that the increase in calcium was because of internal store release.

Fiber Optic Light Guide Measurement in Conjunction with EGTA Shows That the Increase in Internal Calcium Was Not Because of Influx from the Extracellular Media—In order to capture the rapid response of intracellular calcium to UTP and nsPEF in the absence of extracellular calcium, fiber optic light guides were used to monitor fluorescence in the BioSmith cuvettes after stimulation. Fig. 7*A* shows the effect of 10 μM UTP on $[Ca^{2+}]_i$. Each trace represents the mean of four replicates, and Fig. 7*A* represents 1 of 4 separate experiments performed on different days. Consistent with what we observed previously, UTP produced a rapid and prolonged increase in $[Ca^{2+}]_i$ when calcium was present in the medium. When 1.5 mM EGTA was added at zero time, there was an immediate and was an immediate and gradual decline in $[Ca^{2+}]_i$ consistent with previous results (Fig. 6). The addition of UTP at 15 s to cells treated with EGTA at zero time induced a rapid and transient rise in $[Ca^{2+}]_i$ such that by 90 s post-treatment the $[Ca^{2+}]_i$ was back to the pre stimulated base line. These experiments show that in HL-60 cells there is a very small window of time (about 1 min) in which to observe purinergic stimulation of $[Ca^{2+}]_i$ when the extracellular calcium was chelated with EGTA. The data in Fig. 7*B* shows the effect of one 60 ns, 15 kV/cm pulse on $[Ca^{2+}]_i$ in similar calcium deficient conditions. When calcium was present in the extracellular medium, there was a rapid and sustained increase in $[Ca^{2+}]_i$. When EGTA was added to the medium, there was an immediate and steady decline in $[Ca^{2+}]_i$, similar to that seen in Fig. 7*A*. When cells were pulsed at 15 kV/cm in the presence of 1.5 mM EGTA, there was an immediate increase in $[Ca^{2+}]_i$ that began to decrease after ~10 s, and after ~60 s the $[Ca^{2+}]_i$ was

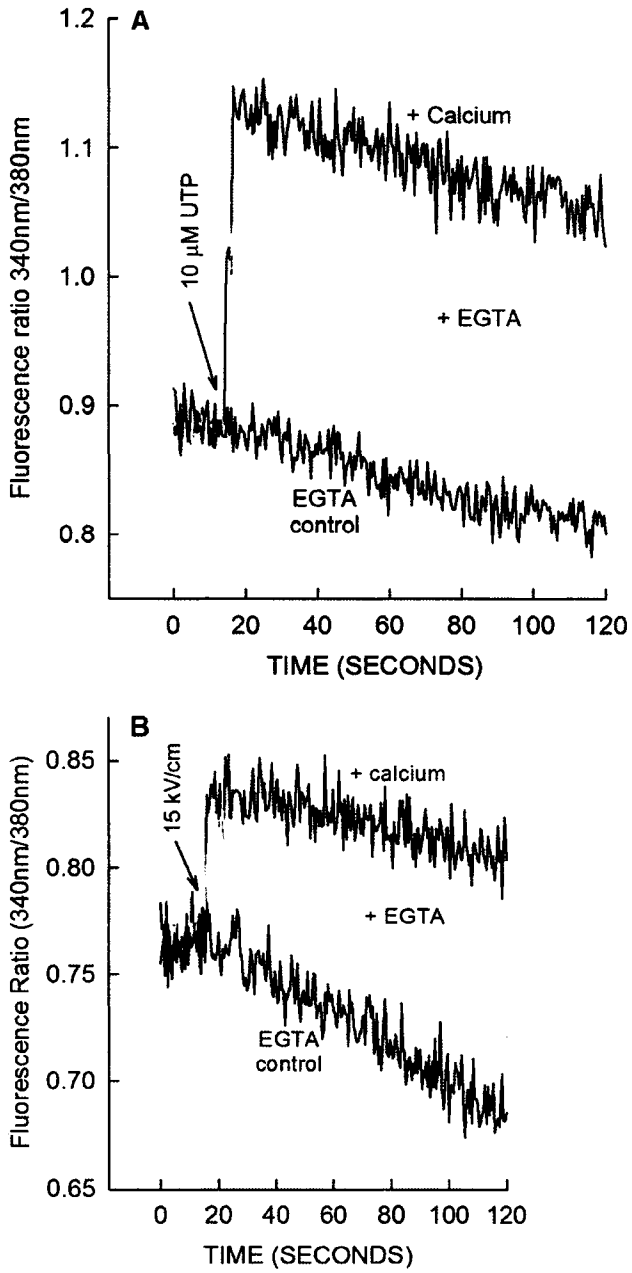

FIG. 7. **Fiber optic light guide allows "capture" of HL-60 response to nsPEF stimulation in the presence of equimolar amounts of EGTA to calcium.** HL-60 cells were treated with 10 µM UTP (*A*) and nsPEF (*B*) in the presence 1.5 mM of calcium. 1.5 mM EGTA was added to the cuvette prior to stimulation to chelate calcium in those experimental traces marked as such. In the presence of EGTA, a response to UTP and to nsPEF is still seen representing calcium release from internal stores. Traces are of a representative experiment (n = 4) and are the average of four replicates within one experiment.

back to base line and continued to decline below base line. The difference in peak heights between the presence of calcium and when EGTA was present was not significant. These data show that nsPEF treatment produces a rapid mobilization of intracellular calcium similar to that observed with UTP (Fig. 7*A*). This method of acquiring fluorescent signals by using a light guide resulted in reliable data; however, it also generated much noise. To reduce this noise level we transferred the HL-60 cell suspension from the BioSmith cuvette to a fluorometry cuvette after treatment, and we continued to measure fluorescence readings. Because this transition took longer than 20 s when we used cell suspension with added EGTA, the calcium response was often missed. Therefore, we continued our experiments in media that contained no added calcium so that the calcium concentration in the media was nominal. This allowed us to capture the increase in internal calcium released from internal stores in response to UTP or nsPEF treatment. Also the data were represented as a 340/380 ratio rather than nM concentrations because mixing of reagents for Fura-2 calibration was difficult with the fiber optic light guide and BioSmith cuvettes.

Effect of Single nsPEF Pulses and Traditional Agonists on HL-60 Cells in Calcium-deficient Media—The amount of calcium released from internal stores and that which entered from the external media was evaluated using the fluorescent indicator Fura-2, which permits $[Ca^{2+}]_i$ to be quantified. These measurements of the response to nsPEF and other agonists could then be compared. The data in Fig. 8*A* show a typical result when cells were pulsed once at 15 kV/cm for 60 ns. In the presence of extracellular calcium, there was a rapid and sustained increase in $[Ca^{2+}]_i$ of ~600 nM. In the absence of extracellular calcium, the basal $[Ca^{2+}]_i$ was lower than when extracellular calcium was present, suggesting that HL-60 cells are not able to completely maintain internal calcium levels in calcium-deficient environments. One 15 kV/cm pulse for 60 ns in the absence of extracellular calcium gradually increased $[Ca^{2+}]_i$ by ~140 nM, which then slowly declined after ~10 s. Because this result is similar to agonist-induced increases in $[Ca^{2+}]_i$ in many different cell types, HL-60 cells in many different cell types, HL-60 cells were challenged with a known agonist that increased $[Ca^{2+}]_i$. UTP was chosen because this has been used previously to elevate $[Ca^{2+}]_i$ in HL-60 cells (13). The data in Fig. 8*B* shows that 10 μM UTP increased $[Ca^{2+}]_i$ by ~300 nM when extracellular calcium was present. This agonist, at 10 μM, produced a rapid and sustained increase in $[Ca^{2+}]_i$ that was of a similar magnitude and duration to that observed with the one 60-ns 10 kV/cm pulse. A 100 μM concentration of UTP did not produce any larger effect on $[Ca^{2+}]_i$, whereas 0.1 μM UTP produced an effect on $[Ca^{2+}]_i$ that was ~20% that seen with 10 μM UTP; thus UTP produced a dose-dependent effect on $[Ca^{2+}]_i$ (Fig. 8*B, inset*). Similar results were obtained using ATP as an agonist (data not shown). In the absence of extracellular calcium, UTP increased $[Ca^{2+}]_i$ by ~50 nM, and the increase in $[Ca^{2+}]_i$

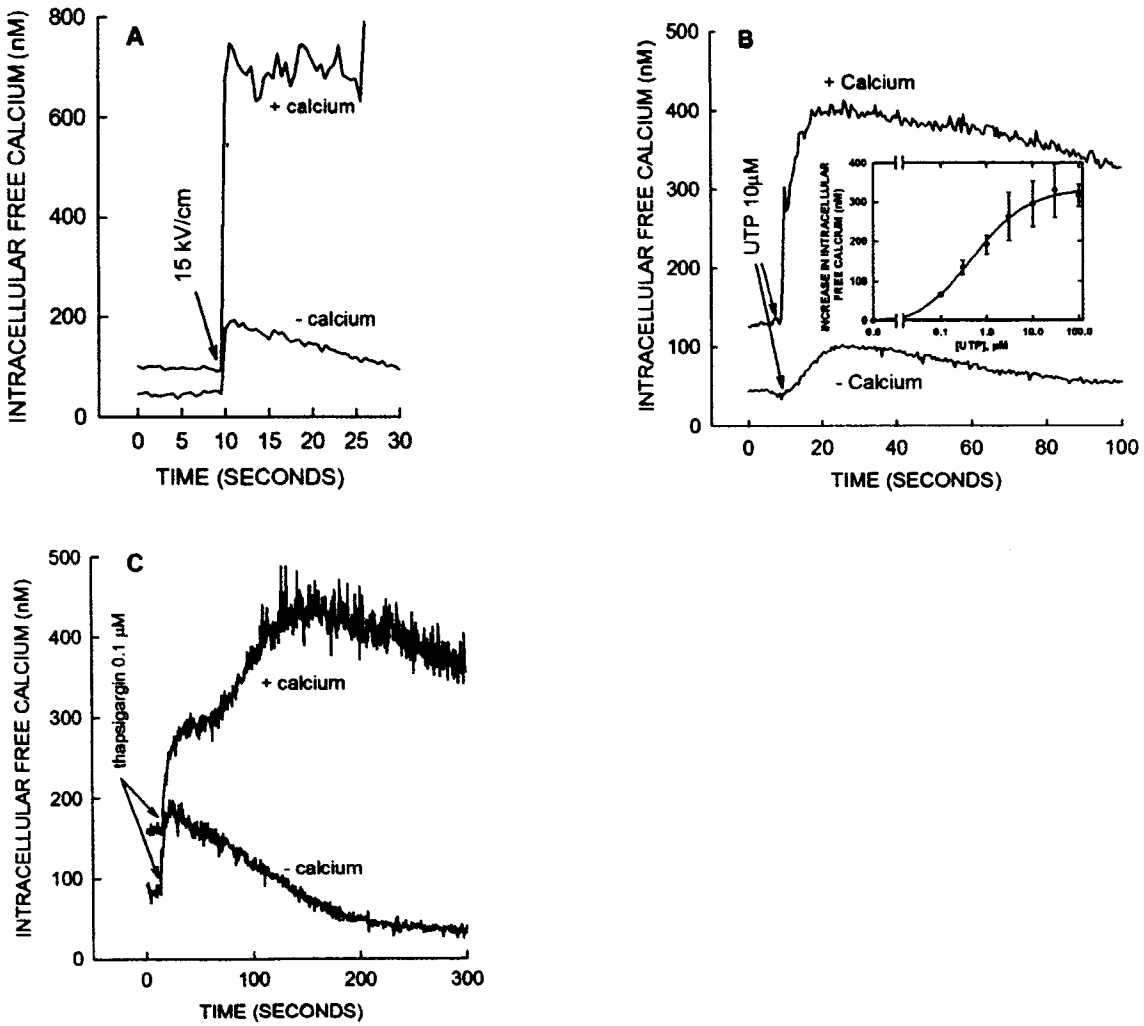

FIG. 8. **Effect of one 60 ns pulse at 15 kV/cm, 10 μM UTP, and 0.1 μM thapsigargin on $[Ca^{2+}]_i$ in Fura-2-loaded HL-60 cells incubated with and without extracellular calcium.** HL-60 cells (incubated with and without extracellular calcium) were placed in the fluorometer cuvette to obtain a base-line $[Ca^{2+}]_i$ value and then were moved into the BioSmith cuvette. The cells were pulsed for 60 ns at 15 kV/cm and then moved back into the fluorometer cuvette, and $[Ca^{2+}]_i$ was again measured (*A*). The effect of 10 μM UTP on $[Ca^{2+}]_i$ was measured in HL-60 cells in the presence and absence of extracellular calcium (*B*). Shown in *B* is a dose-response curve of UTP to increase $[Ca^{2+}]_i$ in HL-60 cells in the presence of extracellular calcium. Various concentrations of UTP were added to Fura-2-loaded cells, and at 15 s the $[Ca^{2+}]_i$ calcium was measured. The effect of 0.1 μM thapsigargin on $[Ca^{2+}]_i$ was measured in HL-60 cells in the presence and absence of extracellular calcium (*C*). Representative traces of at least three experiments are shown.

was transient, consistent with intracellular calcium stores being depleted (56). Because it is believed that purinergic stimulation of HL-60 cells results in an increase of $[Ca^{2+}]_i$ via intracellular calcium mobilization, followed by activation of store-operated calcium channels in the plasma

membrane, thapsigargin was utilized to examine whether or not HL-60 cells possess a store-operated calcium mechanism. The data in Fig. 8*C* show that thapsigargin produced a prolonged increase in $[Ca^{2+}]_i$ when extracellular calcium was present and a smaller and more transient increase in $[Ca^{2+}]_i$ when extracellular calcium was absent. These results are consistent with 60 ns pulses producing an increase in $[Ca^{2+}]_i$ that is comparable with that seen with UTP and thapsigargin and that a store-mediated calcium entry process was involved.

Evidence of Capacitative Calcium Entry Activation in HL-60 Cells—In order to evaluate the activity of CCE, HL-60 cells were treated with nsPEF in calcium-deficient media, and the response of the cells to calcium re-introduction was monitored. The data in Fig. 9*A* shows that when cells were pulsed for 60 ns with an amplitude of 6.4 or 15 kV/cm in calcium-deficient media, there was a small and transient increase in $[Ca^{2+}]_i$ consistent with the data shown in Fig. 8*A*. The 15 kV/cm pulse produced a larger increase in $[Ca^{2+}]_i$ than that seen with the 6.4 kV/cm pulse. When calcium was added to the cells that had been pulsed, there was a rapid rise in $[Ca^{2+}]_i$ consistent with calcium influx channels being activated. The increase in $[Ca^{2+}]_i$ was dependent on the electric field intensity of the pulse because the 15 kV/cm pulse produced a larger increase in $[Ca^{2+}]_i$ than the 6.4 kV/cm pulse (see Fig. 10 for more complete electric field-dependent cell responses), and these increases in $[Ca^{2+}]_i$ were greater than the increase in $[Ca^{2+}]_i$ seen in control (untreated) cells. The data in Fig. 9*B* show that the effect of UTP on $[Ca^{2+}]_i$ is small and transient in low calcium-containing buffer, consistent with the data shown in Fig. 8*B*. The addition of 2 mM calcium to these UTP-treated cells produced a rapid rise in $[Ca^{2+}]_i$ that was comparable with that observed when cells were treated with UTP in calcium-containing media. (Fig. 8*B*) Because UTP has been shown previously to promote capacitative calcium entry in HL-60 cells, the data shown in Fig. 9*B* was entirely consistent with this process. Fig. 9*C* represents the response of HL-60 cells to 0.1 μM thapsigargin incubated in calcium-containing medium and calcium-deficient medium. This figure also illustrates capacitative calcium entry response when calcium (1.5 mM) is re-introduced to thapsigargin-treated cells in a calcium-deficient environment. The results in Fig. 9*A* show that nsPEF treatment of HL-60 cells promotes a stimulation of calcium entry similar to that seen following UTP and thapsigargin stimulation implying that nsPEF treatment was also promoting capacitative calcium entry.

Dose-dependent Increase in $[Ca^{2+}]_i$ *and CCE to nsPEF*—In order to evaluate the electric field dependence of increasing $[Ca^{2+}]_i$ and CCE with nsPEFs, HL-60 cells were treated with nsPEFs at varying electric fields. The data in Fig. 10 show the effect of one 60 ns pulse at various electric field settings in the presence and absence of extracellular calcium. This figure also shows

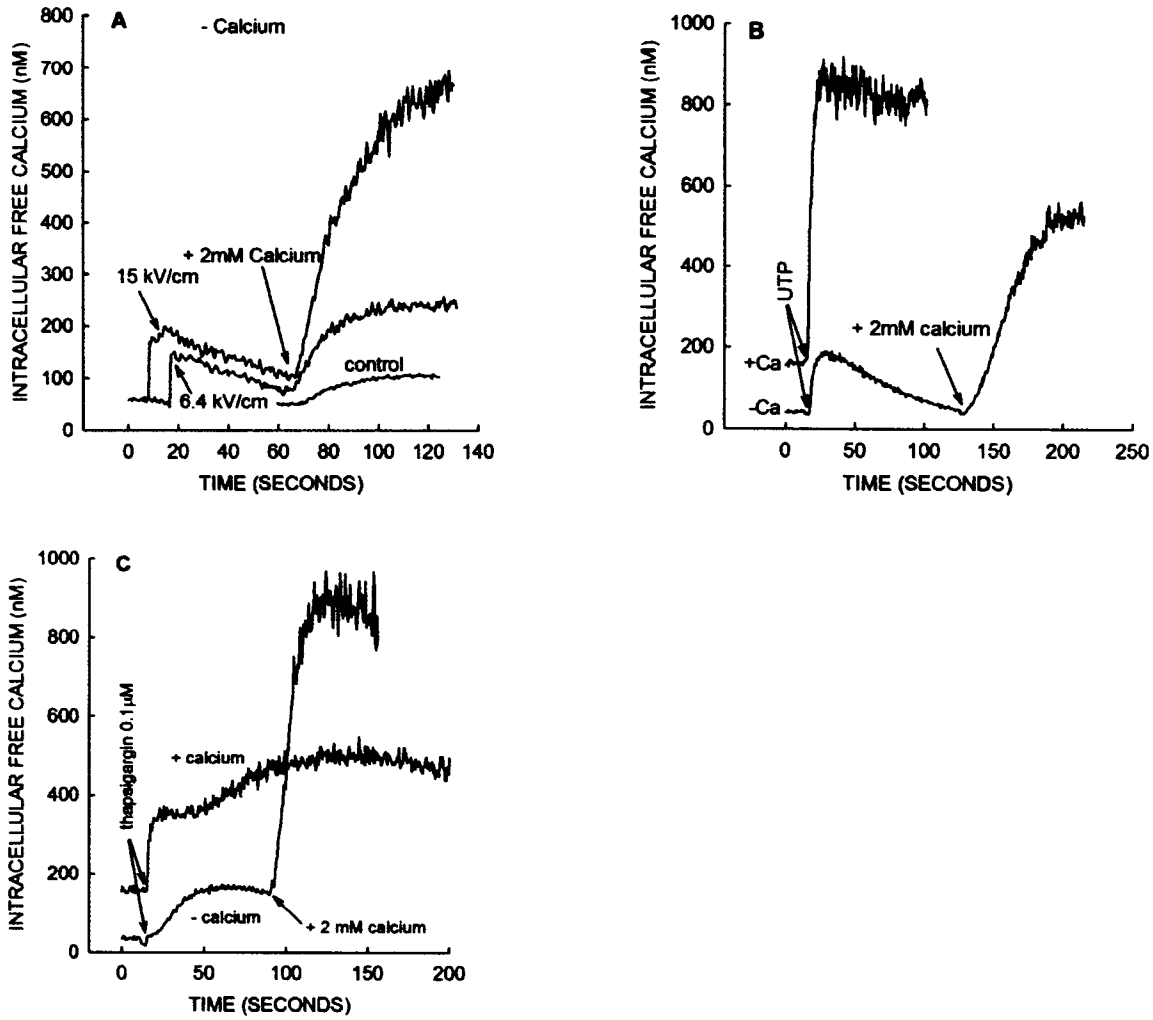

FIG. 9. **Capacitative calcium entry into HL-60 cells treated with one 60 ns pulse each of 6.4 and 15 kV/cm and cells treated with UTP.** HL-60 cells were incubated in the absence of extracellular calcium. Cells, incubated in calcium-deficient media, were treated with one 60-ns pulse at 6.4 and 15 kV/cm. After $[Ca^{2+}]_i$ had returned to near basal values, 2.0 mM calcium was added to the cells (*A*). Untreated cells acted as a control and show that some basal calcium influx occurred in this calcium-deficient situation. Cells were treated with 10 µM UTP, and when $[Ca^{2+}]_i$ had returned to basal values 2 mM calcium was added (*B*). The increase in $[Ca^{2+}]_i$ was similar to that observed when cells were given UTP in the presence of extracellular calcium (Fig. 8*B*). 0.1 µM thapsigargin was also used for comparison to show capacitative calcium influx (*C*). Representative traces of at least three experiments are shown.

the nsPEF effect on $[Ca^{2+}]_i$ of adding extracellular calcium to the media after stimulation as a measure of CCE (see Fig. 9*A* for typical experiment). With calcium present in the extracellular medium, nsPEFs induced an electric field-dependent increase in $[Ca^{2+}]_i$. At 15 kV/cm, the effect

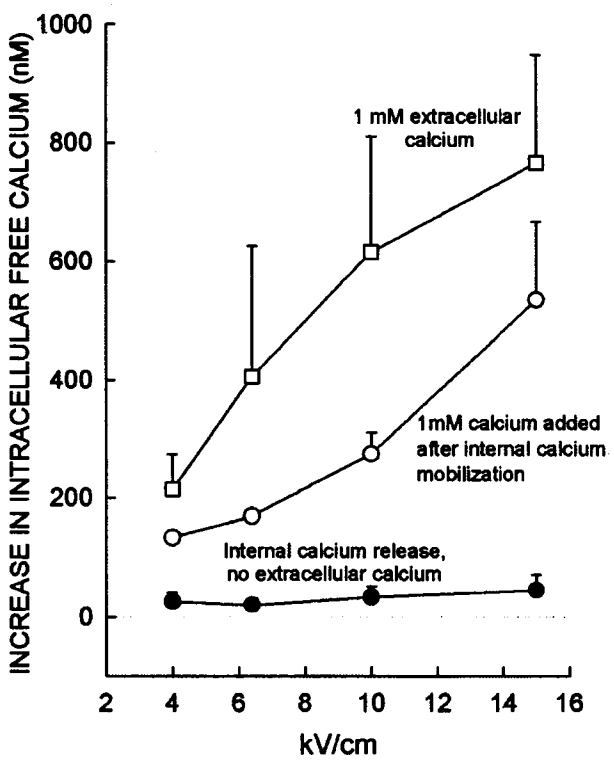

FIG. 10. **Effect of one 60 ns pulse each of 4.0, 6.4, 10.0, and 15.0 kV/cm on $[Ca^{2+}]_i$ in HL-60 cells.** The three conditions shown are as follows: □, when 1.5 mM extracellular calcium was present; ●, in the absence of extracellular calcium; ○, when 2 mM calcium was added to cells after stimulation in the absence of extracellular calcium (see Fig. 8*A* for representative experiment). This represents the entry through the CCE. Data represent the mean ± S.E. from three separate experiments.

on $[Ca^{2+}]_i$ was ~800 nM with one pulse. Because of the high voltage equipment necessary to generate our nsPEF pulses, an increase in electric fields above 15 kV/cm with the 0.4 cm cuvettes risked mechanical breakdown. To counter this, multiple pulses at the 15 kV/cm electric field were administered in attempt to achieve a saturation effect with nsPEF comparable with that seen with 100 μM UTP. Increasing the number of pulses to 3, 5, and 10, separated by approximately 1 s intervals, did not produce any larger effect on $[Ca^{2+}]_i$ than a single 15 kV/cm pulse. However, at lower electric fields increasing the pulse number caused additional increases in intracellular calcium, but not above levels induced by 15 kV/cm (data not shown). An effect of nsPEF on intracellular mobilization was observed (Fig. 10, *solid circles*). However, the maximum effect on

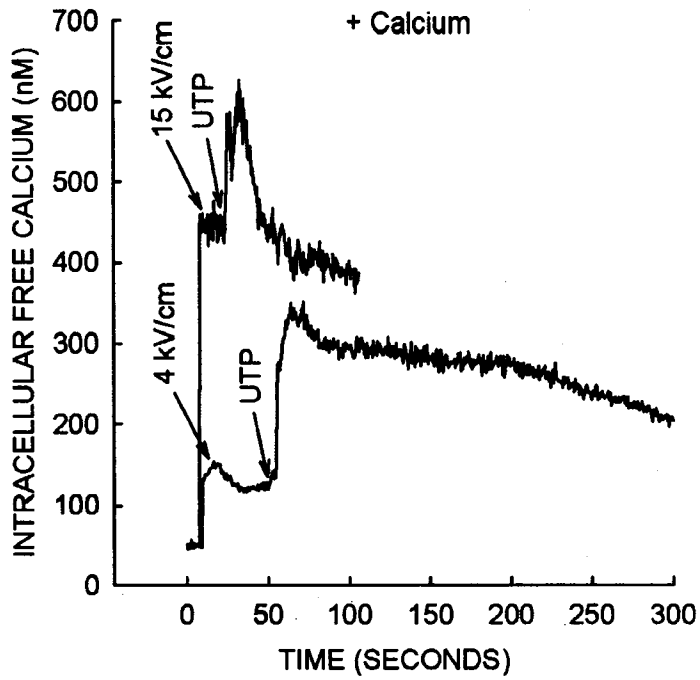

FIG. 11. **Effect of UTP on $[Ca^{2+}]_i$ after one 60 ns pulse each of 4 and 15 kV/cm.** Fura-2 loaded HL-60 cells were incubated in calcium containing media. Cells were either pulsed at 15 or 4 kV/cm. Shortly after nsPEF treatment, the increase in $[Ca^{2+}]_i$ was measured and then 10 μM UTP was added. Representative traces are shown.

$[Ca^{2+}]_i$ was ~50 nM, and this effect was much less than that observed when calcium was present in the medium. However, when calcium was added back to the media of these stimulated cells (Fig. 10, *open circles*), there was an electric field-dependent rapid rise in $[Ca^{2+}]_i$ that approached values similar to those seen when calcium was present during stimulation (Fig. 10, *open squares*). Now that it has been determined that HL-60 cells respond to nsPEF in an electric field-dependent manner, it is important to assess whether or not the nsPEF treatment was depleting the same intracellular stores as UTP.

Effect on $[Ca^{2+}]_i$ in HL-60 Cells Following Sequential Stimulation with UTP and nsPEF—The data in Fig. 11 show the pulse-dependent nature of the increase in $[Ca^{2+}]_i$, with the 15 kV/cm pulse producing an effect ~4 times larger than the effect seen with 4 kV/cm. The data in Fig. 11 indicated that the nsPEF treatment of HL-60 cells was promoting intracellular calcium mobilization and calcium influx via a capacitative influx mechanism similar to the effect of UTP, an agent that also promotes capacitative calcium influx. Therefore, it seemed logical that the in

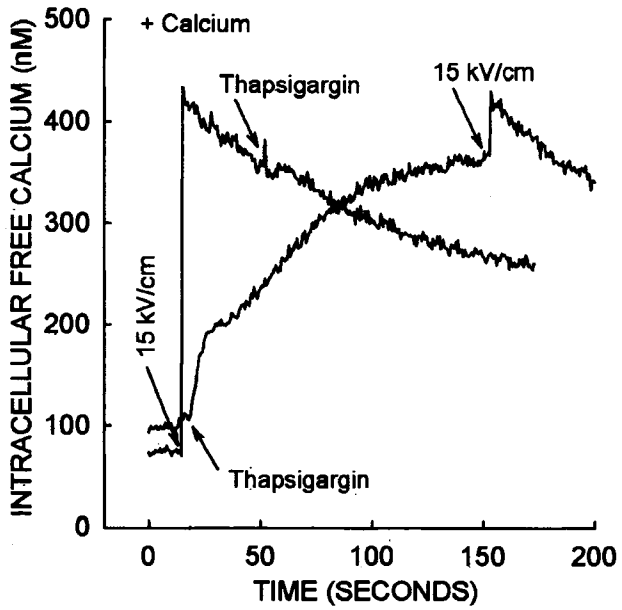

FIG. 12. **Effect of one 60 ns 15 kV/cm pulse followed by 10 μM UTP, and the effect of 10 μM UTP followed by one 60 ns 15 kV/cm pulse on $[Ca^{2+}]_i$ in HL-60 cells incubated in calcium-deficient media and in the presence of 1.5 mM extracellular calcium.** Both the 15 kV/cm pulse and UTP produced a transient increase in $[Ca^{2+}]_i$. The addition of UTP to the 15 kV/cm pulsed cells produced an effect on $[Ca^{2+}]_i$ that was less than that observed when UTP was added alone. Stimulating the cells with one 15 kV/cm pulse after UTP stimulation also produced an effect on $[Ca^{2+}]_i$ that was less than that seen with a pulse alone (*A*). *B*, both the 15 kV/cm pulse and UTP produced rapid and sustained increases in $[Ca^{2+}]_i$. The addition of UTP to the 15 kV/cm pulsed cells produced an effect on $[Ca^{2+}]_i$ that was less than that observed when UTP was added alone to the cells. Stimulating the cells with one 60 ns pulse after UTP stimulation also produced an effect that was less than that observed with one pulse given alone. This heterologous desensitization suggests that both stimuli are mobilizing the same calcium pool. A representative experiment is shown.

crease in $[Ca^{2+}]_i$ induced by UTP would be influenced by prior nsPEF treatment if nsPEFs and UTP were sharing the same capacitative mechanism. When cells were pulsed with 15 kV/cm, the subsequent effect of UTP to increase $[Ca^{2+}]_i$ was greatly reduced, and although there was a very

rapid increase in $[Ca^{2+}]_i$, the effect on $[Ca^{2+}]_i$ was very transient. When cells were pulsed at 4 kV/cm, which produced a smaller increase in $[Ca^{2+}]_i$, the subsequent UTP challenge produced a rapid increase in $[Ca^{2+}]_i$ that was more prolonged in nature. This is similar to the effect seen without prior nsPEF treatment (Fig. 8*B*). Thus the effect of UTP to increase $[Ca^{2+}]_i$ was inversely proportional to the electric field intensity of the pulse. These data suggest that nsPEF treatment and UTP target the same intracellular calcium pools.

In order to more firmly support this hypothesis, the responses of these same types of experiments in the presence of calcium were compared with those in media deficient of calcium. The data in Fig. 12*A* show the effect of one 15 kV/cm pulse on $[Ca^{2+}]_i$ followed by stimulation with UTP and the effect of UTP stimulation on $[Ca^{2+}]_i$ followed by one 15 kV/cm pulse, when extracellular calcium was deficient. One 15 kV/cm pulse produced an increase of ~80 nM, which rapidly declined to a value just above the pre-stimulated level, and at this point (180 s) 10 μM UTP was added. The effect of UTP to increase $[Ca^{2+}]_i$ was much smaller (peak effect reduced by ~66 ± 12% S.E., n = 3) than that observed when UTP was added before a pulse. Thus one pulse appeared to partially deplete the same pool of intracellular calcium that UTP was mobilizing, and this pool was the ER, based on the known signaling pathway for UTP in HL-60 cells. The reverse protocol in which cells were challenged first with UTP and then pulsed was also employed. UTP produced a transient increase in $[Ca^{2+}]_i$, consistent with UTP mobilizing calcium from the ER. Following this mobilization by UTP, cells were stimulated with one 15 kV/cm pulse. The increase in $[Ca^{2+}]_i$ caused by the pulse was reduced by ~68 ± 6% S.E. (n = 3) that produced when cells were pulsed before UTP addition. This experiment was therefore consistent with the notion that nsPEF and UTP were mobilizing calcium from the same intracellular pool, which is most likely the ER.

The data in Fig. 12*B* show the effect of one 15 kV/cm pulse on $[Ca^{2+}]_i$ followed by stimulation with UTP and the effect of UTP stimulation on $[Ca^{2+}]_i$ followed by one 15 kV/cm pulse, when extracellular calcium was present. In this experiment the elevation of $[Ca^{2+}]_i$ induced by nsPEF treatment and UTP was because of both intracellular calcium mobilization (Fig. 12*A*) and calcium influx. The addition of UTP produced a rapid rise in $[Ca^{2+}]_i$ that was much larger than when there was no extra- cellular calcium present (Fig. 12*A*), and then it began to gradually decline. Cells were then pulsed at 15 kV/cm, which produced a rapid increase in $[Ca^{2+}]_i$ which was reduced by ~71 ± 9% S.E. (n = 3) when compared with the effect observed before UTP stimulation. When cells were initially pulsed with 15 kV/cm, a rapid rise in $[Ca^{2+}]_i$ was observed that was comparable with that observed with UTP stimulation by itself. Following this pulse, cells were stimulated with UTP. This effect of UTP was reduced by ~69 ± 6% S.E. (n = 3) when compared

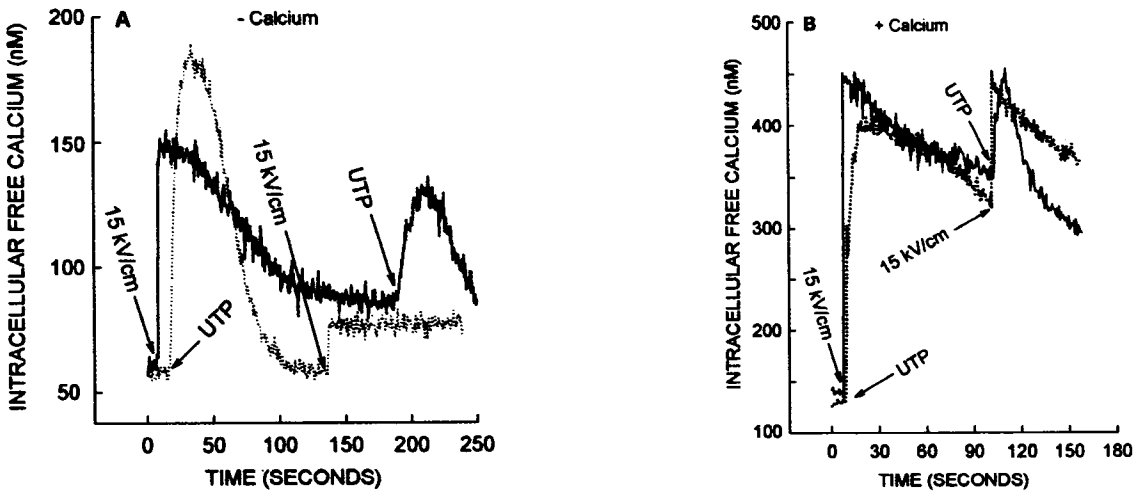

FIG. 13. **Effect of one 60 ns 15 kV/cm pulse followed by 0.1 μM thapsigargin and the effect of 0.1 μM thapsigargin followed by one 60 ns 15 kV/cm pulse on $[Ca^{2+}]_i$ in HL-60 cells incubated in the presence of 1.5 mM extracellular calcium.** The 15 kV/cm pulse produced a large increase in $[Ca^{2+}]_i$ that began to decline gradually; the addition of thapsigargin at 50 s did not increase $[Ca^{2+}]_i$ any further, because the $[Ca^{2+}]_i$ declined at the same rate as before thapsigargin addition. The addition of thapsigargin by itself produced a slow and sustained increase in $[Ca^{2+}]_i$, and nsPEF treatment at 160 s with a 15 kV/cm pulse after thapsigargin produced a small and transient rise in $[Ca^{2+}]_i$. A representative experiment is shown (n = 3).

with the effect of UTP by itself. Therefore, the fact that each previous stimulus reduced the effect of the subsequent stimulus is consistent with the theory that the same signaling pathway was being targeted. This is likely because of release of calcium from the ER.

The data in Fig. 9*A* and Fig. 10 support the concept that 60 ns nsPEF treatment initially mobilized intracellular calcium that then induced CCE. An agent that is commonly used to investigate CCE is thapsigargin (57), which is a potent inhibitor of the sarco-ER Ca^{2+}-ATPases. Treatment of cells with thapsigargin promoted an emptying of the sarco-ER calcium stores with subsequent stimulation of CCE. The data in Fig. 13 show that thapsigargin produced a gradual and sustained increase in $[Ca^{2+}]_i$. If nsPEF treatment depletes the sarco-ER of calcium, then it would be expected that nsPEF treatment after thapsigargin treatment would show a reduced release of calcium when compared with nsPEF treatment alone. The data in Fig. 13 show that the effect of one 15 kV/cm pulse to increase $[Ca^{2+}]_i$ after thapsigargin treatment was reduced by ~63 ± 20% S.E. (n = 3). This result supports the notion that nsPEF treatment and thapsigargin are depleting the same calcium pool, which is believed to be the sarco-ER. The data in Fig. 13 also show the converse experiment in which cells were first pulsed at 15 kV/cm and then challenged

with thapsigargin. The one 15 kV/cm pulse increased $[Ca^{2+}]_i$ to ~400 nM which then began to gradually decline. At ~50 s electrically pulsed cells were challenged with thapsigargin (Fig. 13, *arrow*); however, $[Ca^{2+}]_i$ did not increase and in fact still gradually declined, thus indicating that nsPEF treatment had depleted the thapsigargin-sensitive store of calcium by 100% (n = 3), which is the ER.

DISCUSSION

Recently, investigations of the effects of ultrashort, high intensity pulsed electric fields or nsPEF on mammalian cells have demonstrated distinct differences on cell structure and function compared with classical plasma membrane electroporation. It was demonstrated previously that nsPEF invokes signal transduction mechanisms that initiate apoptosis cascades in several human cell lines (23) including HL-60 cells (27, 21). In the studies reported here, we show that at pulse durations and electric fields that are below the threshold for apoptosis and plasma membrane electroporation, nsPEF recruits signal transduction mechanisms that are similar to those utilized by natural ligands and chemical stimuli. Calcium mobilization induced by nsPEF, purinergic agonists, and thapsigargin exhibit similar kinetics and appear to utilize the same calcium channels present in intracellular and plasma membranes. Specifically, HL-60 cells exposed to nsPEF and UTP exhibited a rapid and transient increase in $[Ca^{2+}]_i$ in the absence of extracellular calcium and a rapid and more sustained increase in $[Ca^{2+}]_i$ in the presence of external calcium. Applications of nsPEF followed by UTP and UTP followed by nsPEF elicited less robust calcium mobilization compared with either stimulus alone, suggesting common sources for calcium mobilization. Based on UTP-stimulated calcium mobilization through PLC and IP_3, the nsPEF-stimulated intracellular calcium channel is expected to be in the ER, and the plasma membrane channel is expected to be a capacitative calcium channel. These CCE channels are likely to be one or more of the TRP channels that are present in HL-60 cells (47). These observations indicate that HL- 60 cells do in fact sense and respond to nsPEF in a fashion that, at least in part, mimics the response seen with naturally occurring stimuli. Based on a simple electric model of the cell and from observations with human cells (1, 8, 21, 23, 27, 53) as the pulse duration is decreased into the submicrosecond range (time domain), effects are less likely to occur on the plasma membrane and more likely to occur on subcellular membranes. Data reported here are consistent with the hypothesis that nsPEFs bypass the plasma membrane and exert effects primarily on internal cellular structures. The absence of PI uptake by cells exposed to nsPEF strongly suggests that calcium does not enter the cells through pores formed by classical plasma membrane electroporation. It could be argued that plasma membrane pores smaller than PI are present, but increases in intra-

cellular calcium were observed in cells in the absence of calcium-containing media and in the presence of EGTA, indicating the release of calcium from intracellular structures. Additional support that nsPEFs affect intracellular structures and functions is provided by the observations that they induced an electric field-dependent increase in capacitative calcium entry when calcium was added to cells in calcium-free media after exposure to the pulse. These findings provide additional evidence that nsPEFs alter intracellular structures without causing plasma membrane electroporation. The increase in $[Ca^{2+}]_i$ in response to nsPEF demonstrates that this method of stimulation bypasses the plasma membrane and targets intracellular structures and functions. The mechanism(s) for HL-60 cell responses to nsPEF stimulation is still unknown, but the data presented suggest this intracellular electromanipulation does increase $[Ca^{2+}]_i$, reaching concentrations that are similar to a natural stimulus such as UTP. Furthermore, calcium elevations appear to reflect classical signaling kinetics. Based on the findings presented here, we pro- pose several possible hypotheses that may explain nsPEF effects on intracellular calcium levels. One possibility is that nsPEF could form transient pores in ER and/or mitochondrial membranes. This would explain the increase in internal calcium levels because calcium would leak out of these organelles down its concentration gradient into the cytoplasm. This theory is supported by the theoretical calculations of Gowrishankar and Weaver (2). The cell could interpret this intracellular calcium mobilization as a naturally occurring signal that then activates CCE in the plasma membrane. Propagation of this calcium signal could then be translated into calcium-mediated cell signaling events including increased gene expression through calcium-dependent transcription promoter mechanisms. The calcium signal could also increase protein translation events that are generally involved in regulation of signal transduction through post-translational modification of proteins. Although ER electroporation remains a possibility, the relatively slow kinetics of calcium mobilization induced by nsPEF and UTP, as opposed to a much more rapid electroporation-induced calcium mobilization, suggests that intracellular membrane electroporation events may not be triggered by nsPEF. A second possibility is that nsPEF pulse could be gating channels directly. Voltage-gated calcium channels could be likely candidates, but they have not been identified in HL-60 cells (58). Furthermore, verapamil and diltiazem, which inhibit voltage-gated calcium channels, had no effect on nsPEF-induced increases in $[Ca^{2+}]_i$ (data not shown). Based on the potential source of the intracellular calcium, IP_3 receptors present in internal membranes are more possible candidates. IP_3 receptors and/or other calcium channels could be triggered by electric field-induced conformational changes that cause the channels to open. Even though the pulse duration is so short and the electric fields are relatively low (below the threshold for apoptosis), effects on conformational changes in proteins are possible. The third possibility is that the nsPEF pulse

could mimic a ligand signal that could trigger receptors on internal membranes thus causing calcium to be released from the internal stores into the cytoplasm. If the cell interpreted nsPEF as a ligand-binding event, then releasing pooled internal calcium would generate the CCE events that were observed. Although effects on intracellular structures and functions are highly likely, additional effects may occur at the plasma membrane that are not measured. For example, nsPEF could trigger activation of the purinergic receptors or G-proteins in the plasma membrane. Alternatively, plasma membrane perturbations could activate PLC or otherwise trigger IP_3 release from membrane, causing calcium release from the ER. Additional studies are required to determine the mechanism(s) for nsPEF-induced calcium mobilization in HL-60 and other cells. Because nsPEFs do not exist in nature, cells have evolved in the absence of these intense electric fields and/or these high frequencies. Nevertheless, the data reported here clearly indicate that cells have sensors that can respond to nsPEF. The data indicate that calcium mobilization does not occur by mechanisms that are related to classical plasma membrane electroporation, but more likely occurs by nsPEF-triggered effects on intracellular structures and functions as we have reported previously (1, 8, 21, 27). The nature of the cell sensor(s) remains to be determined, but it is clear that this sensor(s) is coupled to signal transduction mechanisms that mobilize intracellular calcium in ways that mimic natural ligands in HL-60 cells. nsPEF-induced calcium mobilization is not specific to HL-60 cells but also has been observed in human Jurkat cells and neutrophils, (51, 23). These observations suggest that nsPEFs can be used as stimuli to modulate signal transduction mechanisms that alter cell structure and function and, as shown here, to probe cellular mechanisms for calcium mobilization through intracellular calcium channels and CCE through the plasma membrane.

CHAPTER III

PLASMA MEMBRANE VOLTAGE CHANGES DURING NANOSECOND PULSED ELECTRIC FIELD EXPOSURE

INTRODUCTION

When mammalian cells are placed in a static or slowly varying electric field, charges will accumulate along the plasma membrane and, as a result, the potential difference across the membrane will change from the resting value. The plasma membrane behaves as a leaky dielectric, and when the voltage is increased to ~1 V, water filled pores form in the lipid bilayer resulting in "electroporation" (14, 59). This leads to an increased permeability of the cell membrane (60), allowing for transfer of molecules across the cell membrane. The pore size is a function of the duration of the electric field pulse. Traditional electroporation utilizes pulses microseconds to milliseconds in duration and a few hundred volts to several kilovolts per centimeter. This generates pores large enough for molecules such as DNA to pass through. Current applications of this technique include transfer of genes and drug delivery into cells (34, 61-63). Shorter pulse durations in the nanosecond range are thought to create much smaller pores that will allow ions but not large molecules to pass through (64, 65). At higher electric fields, the probability of creating nonresealable pores increases and, for such pores, cells lose their cytoplasm and die. This effect can be used for food processing (66) or bacterial decontamination (67).

If the rise time of the applied pulsed electric field is faster than the charging time of the plasma membrane, the electric field will pass through the membrane into the cytoplasm and affect internal cell structures. If the amplitude of the applied field is high enough, transmembrane voltages across intracellular membranes will reach threshold values, and pore formation in such membranes becomes likely (8). Although the charging mechanism for intracellular membranes is not yet completely understood, the use of ultrashort pulses on such membranes has been shown to cause a number of new biochemical and biological phenomena. Among the events observed so far are the transient externalization of phosphatidyl serine (68), the release of intracellular calcium (51, 69), and the induction of apoptosis (21, 27).

Better understanding of the effects of pulsed electric fields on membranes requires the measurement of transmembrane voltages in real time, i.e., with a temporal resolution short compared to the charging time of the membrane. Because characteristic charging time constants for the plasma membrane of mammalian cells are on the order of 100 ns, and even less for mem-

branes of subcellular structures (70), realtime measurements require a temporal resolution of 1–10 ns. For larger cells, e.g., sea urchin eggs, where the characteristic membrane charging time constant is in the microsecond range, real-time measurements of membrane charging only require a temporal resolution on the order of 100 ns. Such measurements have been conducted by Kinosita et al. (71) for applied square wave pulses of several microseconds duration and a maximum field strength of 400 V/cm by using a 300 ns laser pulse to excite the voltage sensitive dye, RH292. The advantage of this pulsed illumination with the laser is that the temporal resolution of the measurement is not determined by the shutter time of the camera but by the pulsed (stroboscopic) laser illumination only. The results of the experiments with 400 V/cm pulses showed an exponential increase in the transmembrane voltage until saturation was reached after 2 μs. The saturation of the fluorescence response was assumed to be due to electroporation.

To use the same technique to monitor the transmembrane potential during the exposure to a nanosecond pulsed electric field, a laser pulse of nanosecond pulse duration and a voltage sensitive dye with an equally fast response time are needed. Whereas nanosecond lasers are readily available, only recently has a voltage-sensitive dye, ANNINE-6, with subnanosecond temporal response, become available. ANNINE-6 was developed with a voltage-regulated fluorescence response that depends only on the shift of energy levels due to the Stark effect (72).

To investigate membrane charging in response to an ultrashort pulsed electric field, we stained Jurkat cells with ANNINE-6 and exposed them to an electric field of 95 kV/cm for 60 ns. At different times during the exposure, the cells were illuminated with a laser pulse of 5-ns duration (full-width half-maximum (FWHM)). In this manner, the recorded changes in fluorescence intensity allowed us to monitor temporal development of the transmembrane voltage with a 5 ns temporal resolution.

EXPERIMENTAL PROCEDURES

Cell culture—Jurkat cells, a T-lymphocyte cell line obtained from American Type Culture Collection (Manassas, VA), were cultured in 75 cm^2 flasks in phenol red RPMI 1640 medium (Mediatech Cellgro, Herndon, VA) supplemented with 10% fetal bovine serum (Atlanta Biologicals, Norcross, GA), 1% L-glutamine, and 1% penicillin/streptomycin (Mediatech Cellgro), and incubated at 37°C with 5% CO_2. Cells in log-phase were removed from the culture and resuspended in a physiological buffer before experimentation. The buffer used to resuspend the Jurkat cells was composed of 145 mM NaCl, 5 mM KCl, 0.4 mM NaH_2PO_4, 1 mM $MgSO_4$, 6 mM glucose, 5 mM HEPES, 1.5 mM $CaCl_2$, with enough NaOH added to bring the pH to 7.4.

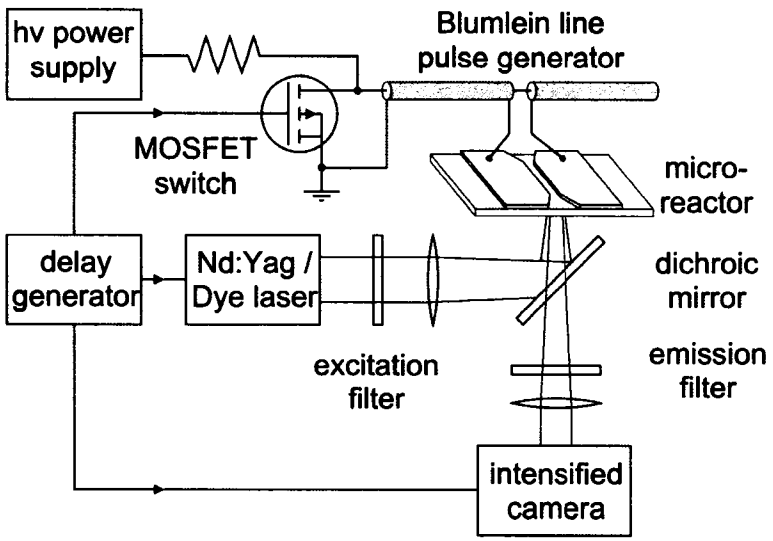

FIG. 14. **Block diagram of the experimental setup**: nanosecond pulse generator, microreactor, and optical system.

Cell staining—Cells were stained with the voltage-sensitive fast response dye ANNINE-6 (Sensitive Dyes GbR, Munich Germany) at a concentration of 16 μM (72). The dye molecules become attached to the cellular membrane, and undergo a change in charge distribution when the voltage across the membrane, or the electric field in the membrane, respectively, is increased. This increase in electric field causes a change in charge distribution of the molecule. This field-induced redistribution occurs on a timescale small compared to nanoseconds, and leads to a shift of the excitation and emission spectra of ANNINE-6. Kuhn and co-workers (73) found strong experimental evidence that the spectral shifts of ANNINE-6 embedded in a plasma membrane depend on the molecular Stark effect (electrochromism) only (74). As a result of the spectral shift, the fluorescence intensity of ANNINE-6 that is observed in a certain wavelength range is modulated strongly by the voltage across the membrane (73) with a response time of ANNINE-6 in the subnanosecond range.

Experimental setup—Stained cells in suspension were placed between two stainless steel electrodes (type 301, Small Parts, Miami Lakes, FL) mounted on a standard (25 X 75 mm) microscope slide. Although some authors doubt the chemical inertness of stainless steel electrodes in experiments with electric fields (75, 76), we have found no adverse effects caused by the material in our experiments thus far. The gap distance between the electrodes is 100 μm (depth and length of the gap are 100 μm and 1 cm, respectively) and the electrodes are affixed to the slide with a <10 μm epoxy layer. A homogeneous electric field was applied to the suspension by means of a

Blumlein line pulse generator matched to the load resistance of the sample between the electrodes (77). The pulse duration is determined by the cable length of the Blumlein line and was set to 60 ns for this experiment. To synchronize the exposure with the pulsed illumination, a fast semiconductor switch (MOSFET (DE275-102N06A, IXYS RF, Fort Collins, CO)) was used as a closing switch for the Blumlein line pulse generator. The MOSFET, which can be triggered with a TTL signal, allows the application of a voltage pulse with amplitude up to 1 kV, corresponding to a maximum electric field in the 100 μm gap of 95 kV/cm. A schematic of the experimental setup is shown in Fig. 14.

The required nanosecond pulsed illumination was accomplished with a dye laser (PDL-2, Quanta Ray, Spectra Physics, Mountain View, CA). The dye laser was pumped by the third harmonic of an Nd:Yag laser (DCR-3, Quanta Ray). Coumarin 440 (Exciton, Dayton, OH) was used in the dye laser to provide illumination at a wavelength close to the excitation maximum of ANNINE-6 at 440 nm. The pulse duration of the multimode laser pulse was 5 ns (FWHM). The laser light is guided through an optical fiber to the microscope, where it is weakly focused on the area between the electrodes of the microreactor on the microscope stage. The diameter of the illuminated spot in the specimen plane is 180 μm. To ensure reproducibility, the laser intensity was adjusted to the same value in each experiment. A filter with an optical transmission peaking at 440 nm and a FWHM of 20 nm prevents excitation of the sample by the laser used to pump the dye laser itself (355, 532, and 1064 nm) and by stray light from sources other than the laser. To further minimize the influence of stray light, the fluorescence emission is observed through a combination of a dichroic mirror and a bandpass filter with a range from 560 to 660 nm. The transmission of this filter is 88 ± 2% over the entire range. The peak laser power density at the illuminated area A = 2.54 X 10^{-4} cm^2, amounts to 5 MW/cm^2. Thus, the peak photon flux density at the specimen plane is I_{peak} = 1.1 X 10^{25} photons per cm^2 and per second. Dye excitation at these moderate power densities is a single-photon process. For two-photon excitation of common fluorescent probes, a photon flux density on the order of 10^{30} cm^{-2} s^{-1} is typically required (78), which is five orders of magnitude higher than is used in the experiment. The laser was operated in single-shot mode triggered by an external signal that was synchronized with the electric field pulse. The timing was controlled with a fast photodiode (S4797, Hamamatsu; Hamamatsu City, Japan). All propagation delays were accounted for and corrected by using appropriate delays on the trigger signals. The principle of the stroboscopic imaging technique is shown in Fig. 15. The voltage pulse applied to the microreactor was trapezoidal with a rise and fall time of ~5 ns (10–90% value). The pulse voltage did not return to zero after 60 ns, but stayed, for another 60 ns, at ~20% of its peak value.

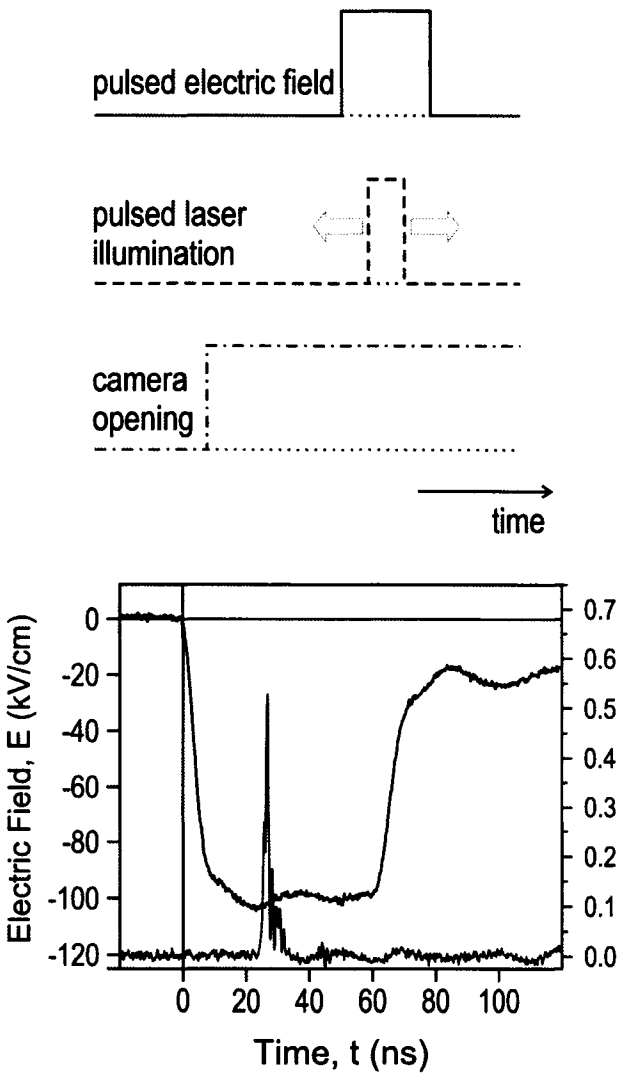

FIG. 15. **Nanosecond Imaging.** The concept of stroboscopic measurements is depicted on the left. The actual laser pulse of 5 ns (recorded with a fast photodiode), relative to the temporal development of the 60 ns applied electric field is shown in the right graphic.

With this system, it is possible to collect images with a temporal resolution of 5 ns, the duration of the laser pulse, by illuminating the cells at different times before, during, and after the 60 ns electrical exposure. It needs to be pointed out, however, that the setup allows the capture of only one image during each exposure to a pulsed electric field. Therefore, the development of the

transmembrane voltage is necessarily a reconstruction from repeated experiments with different cell samples recorded at different times during the electric field exposure.

Fluorescence microscopy—Photographs of the cell sample were taken on an inverted microscope (IX71, Olympus, Melville, NY) with a 600X magnification. A photograph was taken as a reference before the electric field exposure, another during the application of the electric field, and one 30 s after the pulse. The images of the cells were recorded in 12-bit grayscale with a signal amplifying camera (PCO DiCAM Pro, The Cooke Corporation, Auburn Hills, MI). Image processing was done using ImageJ software (National Institutes of Health, rsb.info.nih.gov/ij/). In each image, two to 10 cells were visible between the electrodes. From these cells, a maximum of five cells were analyzed. A circular mask was drawn around each selected cell in the control image taken before exposure to the electrical field, and its dimensions recorded. A smaller circular mask was then drawn to 25% the size of the original and placed at the outermost position (pole) of the membrane facing the cathode and that facing the anode. The average pixel intensity for the selected mask area at both positions was then measured. The same process was repeated for the image taken during the electric field pulse. Background values for each image were subtracted from average pixel intensity values. Once these values were obtained, a ratio of the average fluorescence intensity change in the images, taken before and during the electrical exposure was calculated and expressed as a percentage change in fluorescence intensity. Changes in the fluorescence intensity could be determined with an accuracy of 2%. However, the fluorescence intensity of cells observed in successive experiments with the same exposure parameters varied as much as 12%. The Jurkat cells were stained with a voltage-sensitive dye, ANNINE-6, having a subnanosecond temporal response (73). With a high-intensity laser as excitation source, almost all the dye molecules that are embedded in the membrane will be excited. Because the lifetime of the excited state is on the same order as the laser pulse duration, 5 ns, multiple excitation cycles of the dye molecules are not likely (in contrast to the static illumination by a mercury lamp, where continuous excitation and fluorescent decay occurs). Consequently, for the pulsed laser illumination, the fluorescence signal depends on the number of dye molecules attached to the membrane, rather than on the intensity of the incident light. A laser intensity that is too high results in rapid bleaching of the dye, rendering measurements on transmembrane potential changes futile. To take the influence of laser bleaching into account, we have adjusted the laser intensity to a value that gave us a reproducible fluorescent signal reduction of 80% after 10 laser pulses. In addition, a control image was always taken as the third picture in a sequence of pictures before, during, and after the exposure to the pulsed electric field. The comparison of the fluorescence intensity before and after the application of the electrical pulse, together with the information from images recorded in

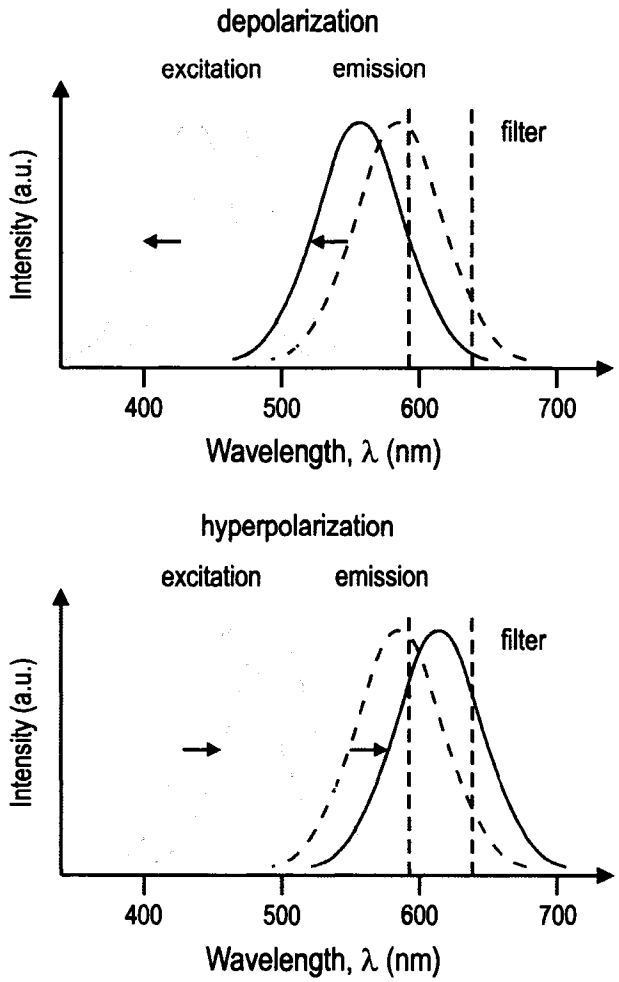

FIG. 16. **Excitation and emission spectra of ANNINE-6.** Spectra are depicted for a resting transmembrane voltage of 50 mV (*dashed curves*). With decreasing voltage across the membrane (depolarization), the spectra are shifted to shorter wavelengths (*solid curves*; diagram on *left*), resulting in a decrease of the light intensity passing through a filter centered at 610 nm with a bandwidth of 100 nm. With increasing transmembrane voltage (hyperpolarization), the spectra are shifted to longer wavelengths (*solid curves*; diagram on *right*), resulting in first, an increase, and, with increasing voltage, a decrease in intensity passing through the filter.

the same sequence but without the effect of an applied electrical pulse, allows us to estimate "inherent" changes in fluorescent intensity that are not caused by changes in the transmembrane

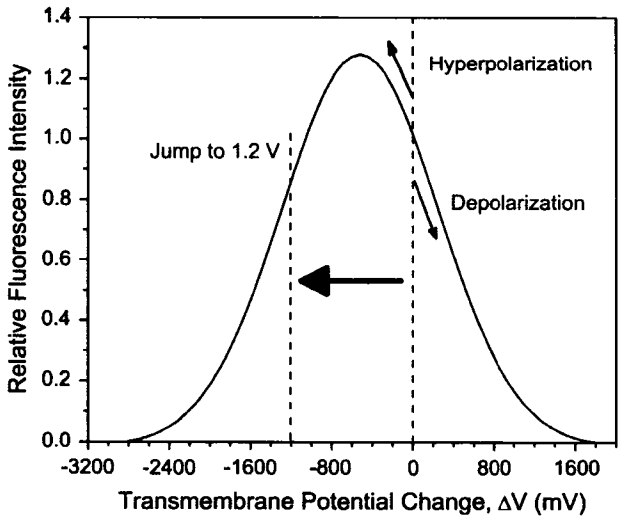

FIG. 17. **The relative fluorescence intensity of ANNINE-6 versus transmembrane voltage change.** The fluorescence has been recorded through a filter centered at 610 nm with a bandwidth of 100 nm and has been normalized with respect to the intensity without electric field application. For a change of the transmembrane voltage at the pole of the cell facing the anode of >1 V the hyperpolarization of the membrane will also lead to a decrease of the fluorescence signal.

voltage. Small fluctuations in the intensity of the laser illumination are responsible for changes in fluorescence of 5–10% between the first and the second image. For a nominal laser energy of 5 μJ (corresponding to a power density of 5 MW/cm^2 at the illuminated focal area), this value was found to be reproducible and was taken into account when the experimental results were evaluated.

Image analysis—When the voltage across the membrane changes due to the applied electric field, the wavelengths for the excitation and emission maxima shift in response (Fig. 16). When the fluorescence signal is observed through an emission filter with a transmission range small compared to the width of the fluorescence emission band, this shift causes a change in the intensity of the recorded signal. With the data provided by Kuhn et al. (79), transmembrane voltages can be calculated from the change in fluorescence intensity as shown in Fig. 17. For an increase of the electric field across the membrane (hyperpolarization), the fluorescence spectrum shifts toward longer wavelengths, corresponding first to an increase in recorded intensity (up to the point where the peak of the fluorescence spectrum coincides with the center wavelength of the

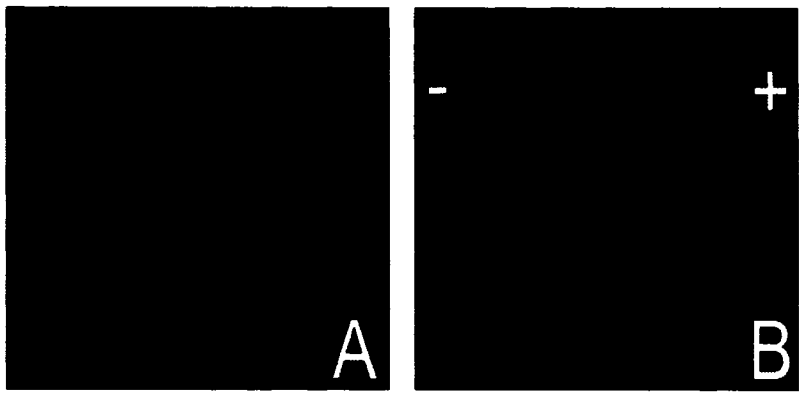

FIG. 18. **Jurkat cells before (*A*) and 25 ns into (*B*) an electric field application.** The images show a drastic decrease of the fluorescence intensity during the pulsed electric field, which indicates high membrane voltages. During the pulse, the intensities are different for the anode- and the cathode-directed hemispheres, but within the hemispheres, are independent of the azimuthal angle θ.

filter transmission), followed by a decrease. The opposite is the case when the electrical field across the membrane decreases (depolarization). The changes in intensity, therefore, provide a measure of the transmembrane voltage.

RESULTS

We have imaged Jurkat cells stained with ANNINE-6 before, during, and after the application of a 60 ns pulse of 95 kV/cm. Images were acquired during the excitation of the dye with a 5 ns laser pulse to achieve a snapshot of the membrane voltage of the entire cell with a 5 ns temporal resolution (Fig. 18). Images acquired before the pulse was applied show a fluorescence distribution that is uniform along the perimeter of the cell, as expected for cells where the voltage across the membrane is just the resting potential difference. For Jurkat cells this is ~50 mV (of negative polarity with respect to the grounded exterior of the cell) (80). When the cells are exposed to high electric fields, the fluorescence decreases dramatically in both hemispheres, slightly more on the hemisphere that faces the cathode (negatively biased electrode) than the hemisphere that faces the anode.

Note that no azimuthal differences in fluorescence intensity can be observed within the same hemisphere of the cell for any time during the exposure. The fluorescence intensity shows only a discontinuity at the equator (perpendicular to the electric field). This indicates that for such high electric fields, the membrane voltage "breaks down" very rapidly, and assumes across each

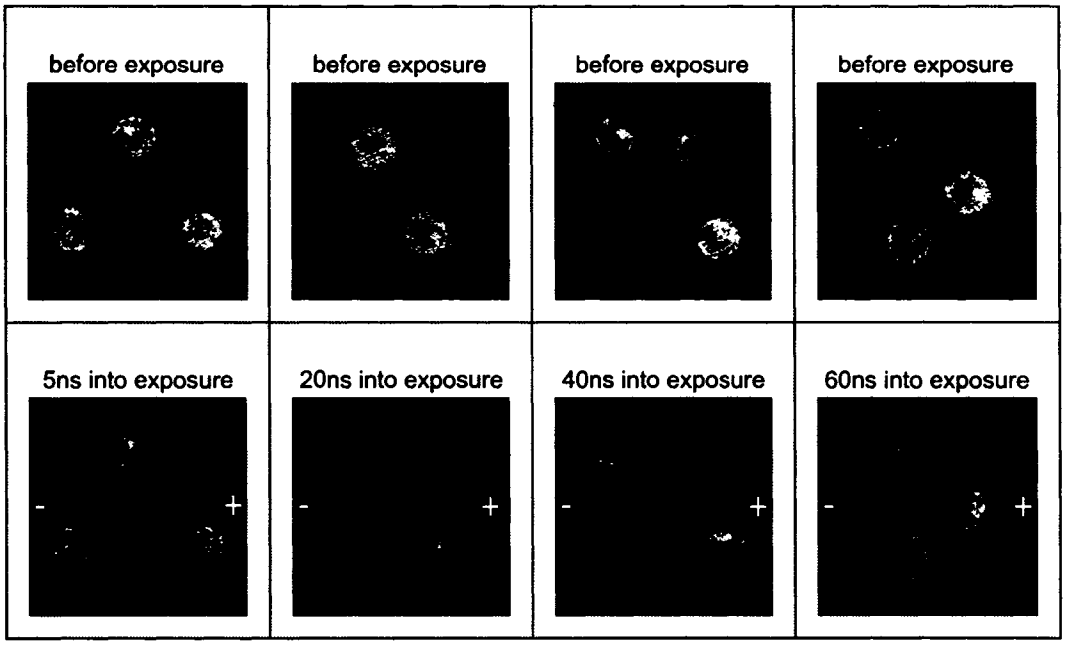

FIG. 19. **Typical images of the fluorescence intensity taken at different times during the exposure.** The external electric field was orientated from the right to the left. Cells were exposed to a 60 ns duration pulse of 95 kV/cm electric field and the images were taken at the times listed. Images taken before the pulse (*top row*) serve as control images.

hemispherical membrane a constant value, which is independent of the azimuth angle, and which is different from computed voltage distribution, where the membrane is considered an ideal dielectric material:

$$\Delta V = 1.5 \cdot E \cdot (D/2) \cdot \cos \theta. \quad (1)$$

D is the cell diameter and θ is the angle with respect to the direction of the applied electric field, E. Similar observations have been made by Kinosita et al. for "conventional" electroporation pulses (71).

The temporal development of the membrane voltage can be recorded by varying the time of illumination with the laser pulse with respect to the applied electric field pulse. For each experiment we acquired a fluorescence image before the pulse, a second image at a single time point during electric field application, and a third image about half a minute after the pulse. Each measurement sequence was performed on a fresh batch of cells that had not been previously exposed to an electric field. A representative set of images is shown in Fig. 19. We then evaluated at

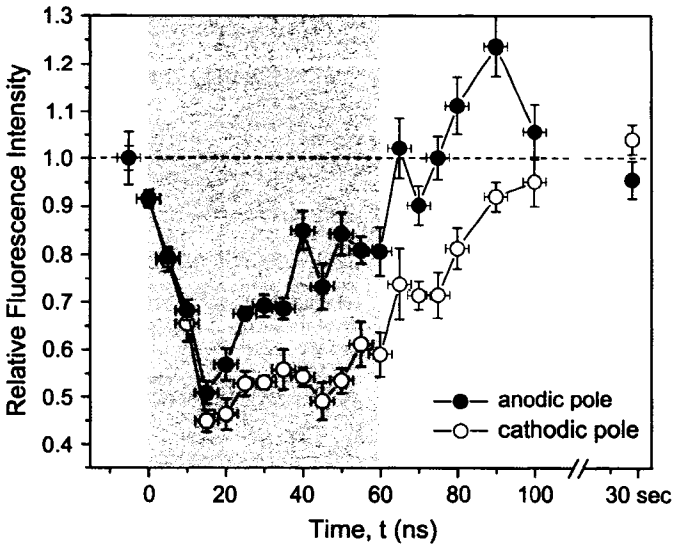

FIG. 20. **Change of the fluorescence signal in response to a change in transmembrane voltage with time.** The data represent the mean fluorescence intensity changes ± SE in three to five experiments. The shaded area depicts the time when the electric field was applied. The change in fluorescence intensity is reaching a maximum at ~15 ns after the electric field is applied.

least five such images, taken at the same time point, from five different cells to determine the average change of the fluorescence signal.

The change in relative fluorescence intensities at the pole of the cell that faces the cathode (negatively biased electrode), and that which faces the anode (positively biased electrode) are plotted versus time in Fig. 20. The gray area depicts the time when the full voltage is applied. The fluorescence intensity rapidly decreases for both the cathodic pole as well as anodic pole, and reaches a minimum ~15 ns after application of the external field. It then increases slightly at the cathodic pole, and more strongly at the anodic pole, during the application of the 60 ns pulse. After the pulse, the intensity increases at an even faster rate than during the 60 ns pulse, and at 30 s, has almost returned to the value of the unperturbed membrane.

Depolarization is expected for the cathode-facing pole of the cell and hyperpolarization for the pole facing the anode. To correlate the observed fluorescence changes with membrane potential we used the bell-shaped calibration curve shown in Fig. 17. The temporal development of the voltage at the anodic and cathodic side of the cells was calculated accordingly as shown in Fig. 21.

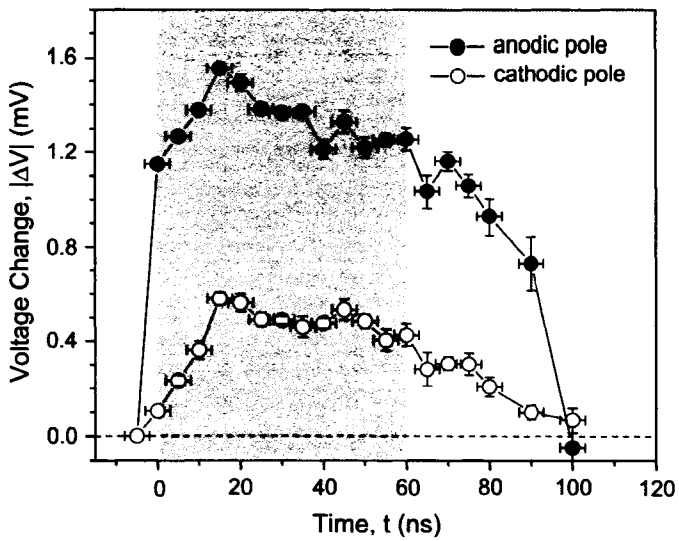

FIG. 21. **Temporal development of the membrane voltage at the cathodic and anodic pole.** The data represent the mean membrane voltages ± SE in three to five experiments. The shaded area depicts the time when the electric field was applied.

We want to point out that the transmembrane voltages, obtained from the fluorescence data, are extrapolated from the available data on the fluorescence response of ANNINE-6, and this extrapolation could be a cause of deviations of the calculated membrane voltage from the real one. Eventually, an experimental calibration of the dye response will be necessary. The design of such measurements for voltages in excess of 1 V is challenging, because independent methods to quantify the membrane potential, such as patch-clamp, require applying very high voltages across the cell for at least several microseconds. Under these conditions, however, the formation of large pores, i.e., "conventional" electroporation of the membrane, is inevitable.

The voltage across the membrane at the anodic pole rises in <5 ns (the temporal resolution of our method) to values of 1.2 V, and then increases at a slower rate of 30 mV/ns to values of 1.6 V, 15 ns after pulse application. During the same time period, the voltage across the membrane at the cathodic pole rises with a rate of ~40 mV/ns to a value of 0.6 V. From 15 ns forward, up to the end of the 60 ns high voltage pulse, the membrane voltages decrease slightly. After the electrical pulse, the voltages at both hemispheres return to the resting voltage.

DISCUSSION

For ANNINE-6, experimental data on the spectral shift of excitation and emission spectra with voltage are available for transmembrane voltage changes up to ±300 mV, although for a different cell line (79). The shift in wave number was found to be 163 cm^{-1} for excitation and 170 cm^{-1} for emission for a change in voltage of 100 mV independent of polarity. We have used these data to calculate the expected response for an excitation wavelength of 440 nm and a range of emission from 560 to 660 nm. The response of the camera in this wavelength range is almost linear as long as the number of counts per pixel is kept on the order of 1000. Consequently a deconvolution with the camera sensitivity curve has a negligible effect on the calibration of voltage change against fluorescence. We can assume that the spectral shift per 100 mV stays the same for voltages in excess of ±300 mV because the fluorescence response caused by the underlying linear Stark effect is not limited to lower voltages. Only for electric fields of >30 MV/cm, do higher order contributions of the field strength become significant in their effect on the shift of electronic energy levels (81). The calculations result in a bell-shaped calibration curve (Fig. 17) where the fluorescence intensity was normalized to one for the undisturbed membrane ($\Delta V = 0$). The observed decrease of fluorescence of the cathode facing side is consistent with the predicted change for depolarization (Fig. 17). The fluorescence intensity is expected to decrease continuously with voltage. For the anode facing pole, one would expect that at the beginning of the pulse, the fluorescence would increase up to 600 mV, the membrane voltage that corresponds to the peak in the calibration curve (Fig. 17) before decreasing again. However, for the 60 ns, 95 kV/cm electrical exposure, an increase in fluorescence intensity was observed only after the end of the 60 ns electric field pulse. This is at a time when the applied electric field has already declined to a value of ~20 kV/cm.

For every other time during the electric field exposure, both hemispheres of the cells show a decrease in fluorescence intensity. For the hemisphere facing the cathode, values as low as 45% are measured ~15 ns after the onset of the pulsed electric field. The value for the hemisphere on the anode side decreases, at the same time, by ~50%. That the expected increase in fluorescence at the anode side during charging was not observed can be explained by the extremely fast rise in membrane voltage, which occurs on a timescale of <5 ns, the resolution of the diagnostic system. Considering that, with a 95 kV/cm electric field applied, the voltage across a 16 μm-diameter cell (the average size of cells in our experiments) reaches 160 V, and that the charging time constant for such a cell embedded in a medium with a conductivity of 1 S/m, and cytosol conductivity of the same value, is on the order of 120 ns, the membrane potential is expected to reach values of 1.2 V (level of fluorescence intensity equal to that with no electric field

applied) in ~1 ns, assuming that there are no changes in the electrical properties of the membrane during this time. With a 5 ns optical exposure time, we would not observe the corresponding initial increase in fluorescence. After the initial rise in voltage at the anodic pole, the cell membrane becomes permeable (as indicated by the change in the rate of voltage increase), but probably only for small, monovalent or divalent ions. Larger molecules such as propidium iodide were not found to enter the cell when 10 ns pulses of about the same amplitude (80 kV/cm) as our 60 ns pulses were applied to HL-60 cells (64). A possible explanation might be that during the first 15 ns the electric field creates a multitude of small nanopores across the cell membrane previously referred to as "supra-electroporation" (82). The small pore size, coupled with the formation of a screened double layer (an effective depletion zone around the pore periphery) limits the membrane conductivity and ionic throughput. Previous molecular dynamic simulations by our group (65) have demonstrated that nanopore formation can occur within the first 10 ns at these electric field strengths, and validates their nanoscale size. The lower transmembrane voltage at the cathodic pole in Fig. 21 suggests that the corresponding conduction current must be larger at this end, implying a polarity dependent asymmetry in electrical transport. There is theoretical (83) and experimental evidence (84) that the anode and cathode sides of cell membranes react very differently to the application of an electric field. Asymmetric pore formation in cell membranes was first reported for plant mesophyll protoplasts by Mehrle et al. (85) who attributed this phenomenon to a superposition of the induced and the resting potentials. It has also been observed for several mammalian cell lines (84, 86) and for vesicles (87). Using microsecond, monopolar pulses, transport of various fluorescent markers across anode- and cathode-facing membranes implied a higher density of small pores at the anode side than at the cathode side. Assuming a similar asymmetry for nanosecond pulses, the differences in pore density and size on anode- and cathode-facing membrane must affect the membrane voltage at constant current. It is therefore reasonable to assume that the relatively low voltage across the cathode-facing membrane, which we obtain from our measurements, is due to a strong asymmetry of the ionic transport parameters. Such an asymmetry in conduction mechanisms at the two opposite poles could be due to formation of cylindrical nanopores with nonuniform cross section. Such pores produce an asymmetric potential profile within the pore region as discussed recently in articles by Siwy et al. (88, 89). This asymmetric potential then leads to nonlinear current-voltage characteristics resembling an electrical diode. The role of asymmetric potentials in facilitating and modifying electrical transport is not new, and had been discussed by Astumian in the context of molecular Brownian ratchets (90). Field-driven translocation of phospholipids might also contribute to an asymmetric potential distribution at opposite hemispheres. Depending on their charge, membrane-embedded

molecules will either be driven into the cell or pulled out into the outer leaflet of the membrane. Recent experiments (68) suggest the translocation of phosphatidyl serine during the application of one pulse of >30 kV/cm and duration of 30 ns. As a result of a significant change in membrane surface, charges inside and outside the cell will affect the transmembrane voltage. The expected azimuthal effect on the transmembrane voltage change was not observed in our experiments. Simplified calculations show that the movement of heavy phospholipids through the membrane in large numbers for an applied electric field for pulse durations of <100 ns cannot be explained by the assumption of an electric force acting on the molecules against the friction in the lipid bilayer alone. This was also demonstrated by recent molecular dynamics studies (91) showing that phosphatidyl serine externalization is a pore-mediated event rather than a direct migration through the membrane. The observed asymmetry in transmembrane potential voltages can be explained by an extended screening layer caused by an increase in phosphatidyl serine molecules around the pore on the anode side. Moreover, the simulations demonstrate that the pulse initiates a pore dynamic that will eventually lead to the formation of pores long after (as compared to the pulse duration) the exposure, which will allow not only small ions to pass, but also larger dye molecules. In fact, the experiments mentioned above (68) and work conducted with longer pulses (92) suggest that, with every pulse, the membrane is altered in a way that facilitates phospholipid translocation. As a consequence, an ongoing increase in translocated molecules can still be observed up to milliseconds, or even minutes, after the exposure. A possible explanation for this alteration might be the uptake of water into the membrane, as, for example, in nanopores. One could presume that another possible reason for the unexpectedly large difference in the calculated anodic and cathodic pole membrane voltage is the assumption that the Stark effect is purely linear. Theoretical studies predict relevant contributions to the shift of energy levels of the dye molecule from the quadratic Stark effect only for electric fields of >30 MV/cm (81) or at least 10 MV/cm (74). Even, if we assume that the membrane is charged to 2 V, the electric field in a cell membrane with a thickness of 5 nm is still only 4 MV/cm, which is too low to expect significant contributions from the quadratic Stark effect that would affect the fluorescence response of the dye. Unfortunately, a calibration of the dye response for transmembrane voltages of 2 V is difficult, if not impossible, because such voltages cannot be applied long enough to the membrane without the formation of pores. Another very important conclusion drawn from these results is the fact that during the pulse, almost all the voltage across the cell appears across the interior of the cell after conduction pores through the membrane have formed. The voltage drop across the membranes can almost be neglected during this time. That means that the cell interior sees approximately the same electric field as the entire cell: 95 kV/cm. It is reasonable to assume that these high electric

fields charge subcellular membranes in the same way as external electric fields charge the outer membrane, and indeed, this "electroporation effect" on subcellular membranes has been observed (8), and is the focus of a large number of current studies (70).

CHAPTER IV

PLASMA MEMBRANE CHARGING OF JURKAT CELLS BY NANOSECOND PULSED ELECTRIC FIELDS

INTRODUCTION

With pulsed electric fields of nanosecond duration it is now possible to instigate specific cell responses, such as apoptosis, release of signaling molecules, progression into the next stage of the cell cycle, etc. (93, 94) These effects depend on specific pulse parameters, which include pulse shape, duration, rise time, and the intensity (voltage) and number of pulses (frequency). It is proposed that the eventual physiological response is due to the preceding, dramatic, albeit transient, changes in membrane potentials, both extra- and intracellular. (95-98) For different exposure parameters different charging mechanisms will be predominant and as a result will allow us to reach different event-thresholds. (99) With conventional electroporation pulses, of several microseconds and field strengths of only a few hundred volts per centimeter, it is generally believed that only the plasma membrane is affected. (13) After reaching a cell-specific threshold, predicted to be on the order of 1 V, the formation of conductive membrane defects in the plasma membrane is anticipated. (13) The permeabilization of the membrane is generally ascribed to pores, which reseal in seconds to minutes after removal of the applied field. (13) With fast rising electric fields of shorter duration, termed nanosecond pulsed electric fields (nsPEFs), sub-cellular structures will also be exposed to the applied field and for high field strengths their membranes can be charged significantly. (22, 23, 69, 100) We believe that reaching different cellular transmembrane voltage thresholds is responsible for the various cell responses observed. These secondary mechanisms after exposure are currently being studied, but as of yet are far from complete. For the induction of apoptosis several studies have already identified pulse parameter thresholds. (21, 102) This recently led to the development of a treatment for melanoma that resulted in the arrest and demise of tumors in mice. (28)

Whereas the physiological cell responses can be investigated with standard diagnostic techniques such as microscopy, histology, or flow cytometry (21, 23, 28), the study of the immediate interaction between the pulsed electric field and the cell requires diagnostics with a temporal resolution that is short compared to the duration of the exposure. We recently reported on the first real-time measurements of transmembrane potential changes for cells exposed to nsPEFs (103). Changes in the fluorescence response of the voltage sensitive, fast response dye, ANNINE-6,

were recorded with a temporal resolution of 5 ns. In this paper, we present an extended study on changes in the charging of the outer membrane as the strength of the applied electric field is varied. A direct physiological effect of the electric field, although unlikely for the short-term exposure, was evaluated by the use of different ion channel blockers.

EXPERIMENTAL PROCEDURES

Cell Culture—Jurkat cells, a T-lymphocyte cell line, obtained from American Type Culture Collection (ATCC, Manassas, VA) were cultured in 75 cm^2 flasks in phenol red RPMI 1640 medium (Mediatech Cellgro, Herndon, VA) supplemented with 10% fetal bovine serum (Atlanta Biologicals, Norcross, GA), 1% L-glutamine, and 1% penicillin/streptomycin (Mediatech Cellgro, Herndon, VA) and incubated at 37 °C with 5% CO_2. Cells in log-phase were removed from the culture and re-suspended in a physiological buffer prior to experimentation. The resuspension solution for Jurkat cells, unless otherwise noted, contained in mM: NaCl, 145, KCl, 5, NaH_2PO_4, 0.4, $MgSO_4$, 1, Glucose, 6, HEPES, 5 (pH 7.4 with NaOH), $CaCl_2$, 1.5.

Cell Staining—Cells were stained with the voltage-sensitive, fast-response dye, ANNINE-6 (Sensitive Dyes GbR, Germany) at a concentration of 16 μM as previously described by Frey et al. (103)

Experimental Setup—Details of the experimental setup have been described elsewhere. (103) Briefly, a homogeneous electric field was applied to the Jurkat cell suspension by means of a Blumlein line pulse generator matched to the load resistance of the sample between two stainless steel electrodes.

Fluorescence Microscopy and Image Analysis—Photographs of the Jurkat cells were taken on an inverted microscope (Olympus IX71, Melville, NY) with 600X magnification. A reference picture was taken before the electric field exposure and another during the application of the electric field. Images of the cells were recorded in 12-bit grayscale with a signal-amplifying camera (PCO DiCAM Pro, The Cooke Corporation, Auburn Hills, MI). The images were processed with a program developed in MatLab (The MathWorks, Inc., Natick, MA). In each set of corresponding photographs, taken before and during the exposure, the cells were outlined with circular masks of radius r. The value of r varies with cell size but was kept the same for the same cell in corresponding photographs. Circles with a radius of 0.25 r were placed on the cell-perimeter at the pole facing the anode (3 o'clock) and the cathode (9 o'clock) at a distance of 0.75 r from the center of the cell. After background intensities were subtracted, the relative average change in fluorescence pixel intensities $\Delta F/F_0$ ($\Delta F = F_e - F_0$, F_e: intensity during exposure, F_0: intensity before exposure) was calculated for the respective areas of interest. The relatively low

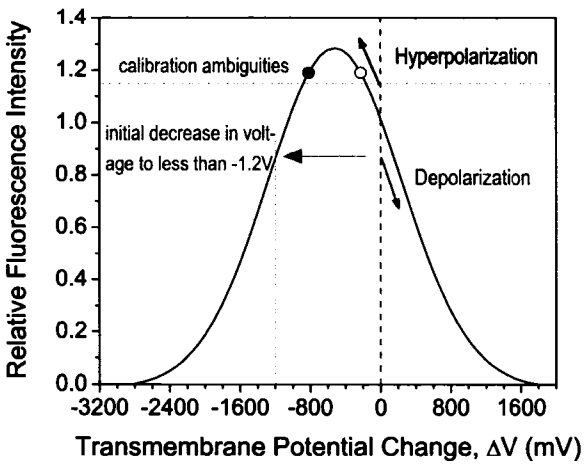

FIG. 22. **ANNINE-6 calibration curve as determined by Kuhn and Fromherz.** (103) For a decrease in the fluorescence signal a transmembrane voltage change can be assigned for the depolarized and hyperpolarized hemisphere. However, relative changes of more than 100%, i.e. an increase in intensity, can be caused by two alternative voltages. An example is given by the empty and filled circle in the figure. Although the fluorescence intensity is the same for both data points the corresponding voltage differs by approximately 600 mV.

standard error of our measurements is due to the time resolution of our experiments being sub-physiological and not necessarily dependent on the age or condition of the cell being analyzed.

Voltage Calibration—A calibration of the fluorescence intensity changes with transmembrane voltage was extrapolated from data on the fluorescence response of ANNINE-6 previously published by Kuhn et al. (79) The calibration curve is shown in Fig. 22. A more detailed discussion of this calibration is given elsewhere. (103)

RESULTS

In order to analyze charging and discharge mechanisms of cell membranes exposed to nsPEFs we stained Jurkat cells with the fast response, voltage sensitive dye, ANNINE-6. Pulsed electric fields of 60 ns were applied with different field strengths of 5, 12.5, 50, and 90 kV/cm. For each set of conditions the development of fluorescence intensity was reconstructed from separate experiments where the change in fluorescence intensity was recorded at 5 ns intervals

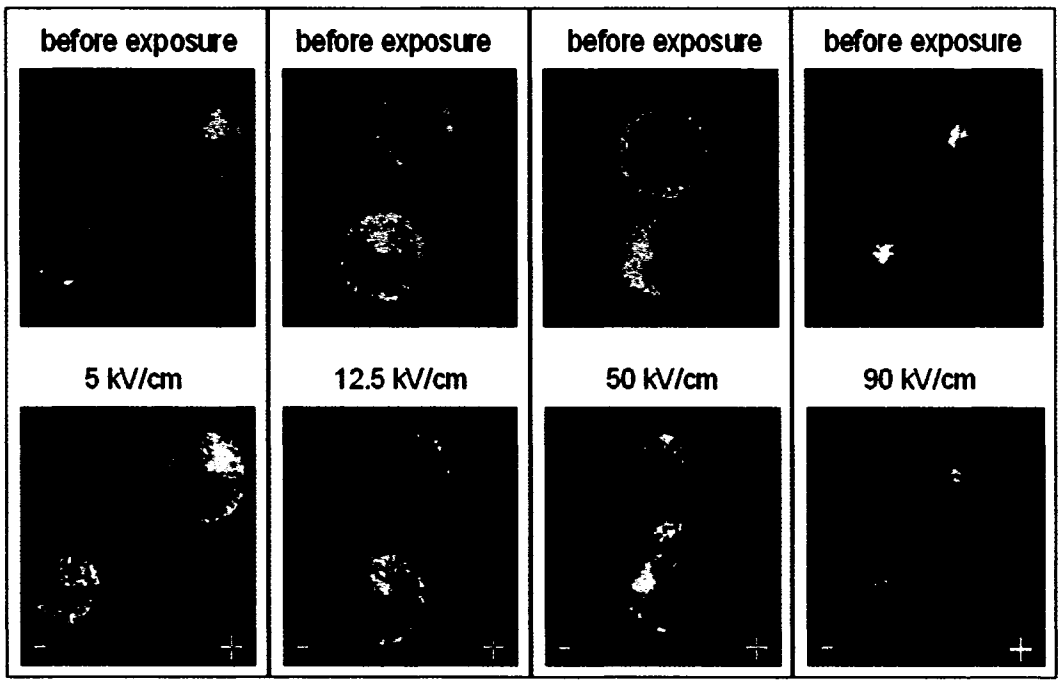

FIG. 23. **Typical images of ANNINE-6-stained-Jurkat cells taken 15 ns into either a 90, 50, 12.5, or 5 kV/cm electric field pulse of 60 ns duration.** The position of the electrodes is depicted with the anode to the right and the cathode to the left of each frame. Each top and bottom image pair is a unique experiment. For the same time during electric field application, 15ns, stronger changes of the fluorescence emission are observed for higher field strengths. This corresponds to a higher transmembrane voltage change of the plasma membrane.

from 10 ns before the pulse was applied, throughout the pulse, and up to 240 ns after the pulse. An example of the field dependent response at a time of 15 ns into the exposure is shown in Fig. 23 for different field strengths. The change in the fluorescence intensity is of greater magnitude as higher electric field strengths are applied, indicating that a higher transmembrane voltage is reached. Notice that there is no obvious angular dependency along the cell membrane. The fluorescence intensity shows only a discontinuity at the equator (perpendicular to the electric field). As mentioned in our earlier publication this is the result of a uniform "break down" of the membrane due to the high electric field strength that is applied. Consequently the transmembrane voltage is the same across hemispheres although the value is different between the anodic and the cathodic side. (104) For the applied field strengths presented here, the voltage at the anodic pole changes very fast and moderate transient voltages that would correspond to an increase in fluorescence intensity could not be captured within the 5 ns resolution limit of our method. Instead,

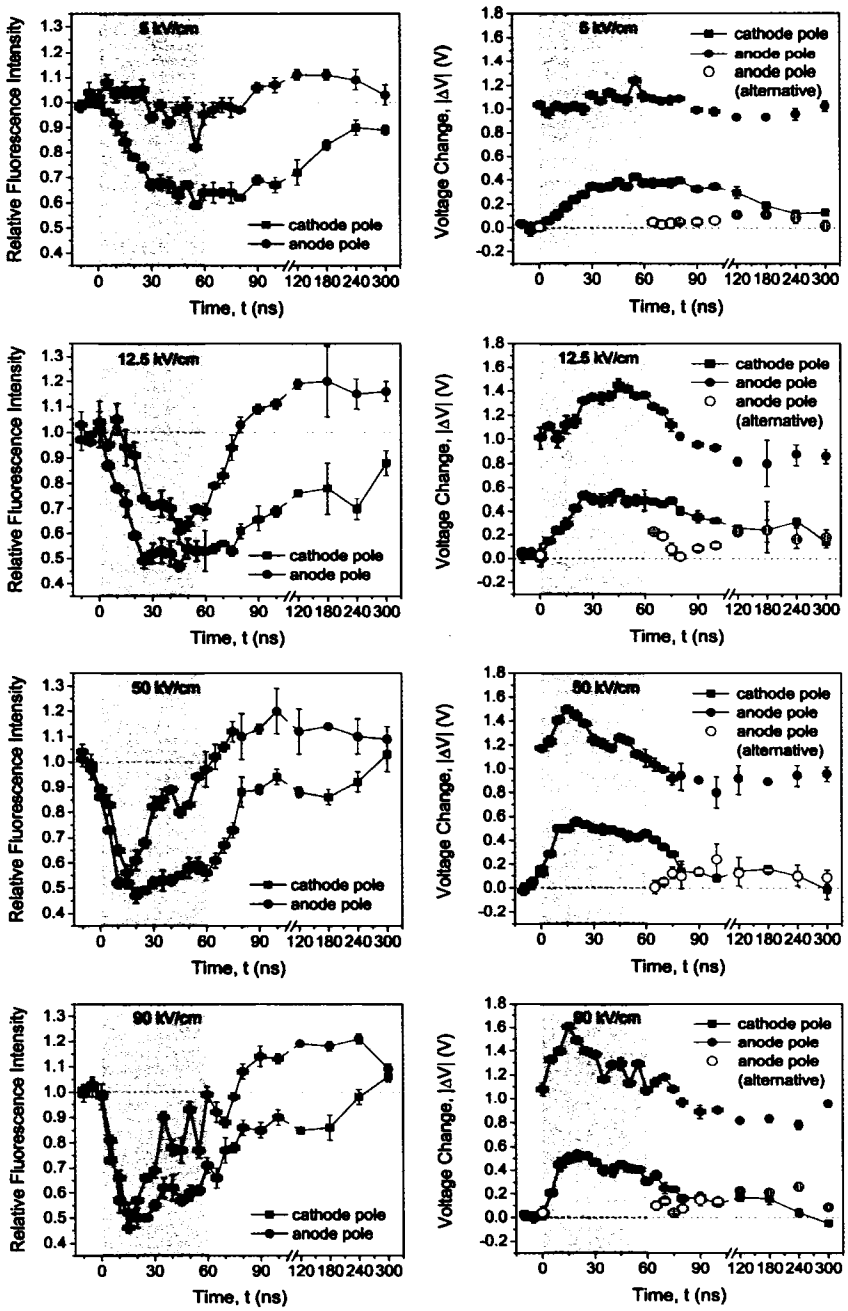

FIG. 24. **Jurkat cells stained with the voltage-sensitive dye, ANNINE-6, show a change in relative fluorescence intensity (left column) in response to nsPEF treatment.** The change in fluorescence intensity reflects a change in transmembrane potential (right column). Each pair, i.e. 1A and 1B, represents the relative fluorescence intensity and transmembrane potential data for one electric field. The electric fields that were applied are as follows: 1) 5, 2) 12.5, 3) 50, and 4) 90 kV/cm. The shaded area depicts the time when the 60 ns duration electric field was applied. Alternative voltage values are presented as open red circles and a line is drawn between the two voltage extrapolation values. Average values represent an n of 5 ± SE bars.

the observed immediate decrease of the fluorescence intensity at both poles of the cell indicates a fast rise in the transmembrane voltage with a change of more than 1 V occurring at the anodic pole.

The relative changes of the fluorescence signal for different times during exposure to electric fields of different strengths are shown in the left column of Fig. 24. The right column shows the transmembrane voltages that can be derived from the recorded fluorescence intensity changes according to the calibration presented in Fig. 22. For measurements close to the maximum of the calibration curve the analysis of the data provides ambiguous results. In the vicinity of this maximum (relative fluorescence intensity greater than 1.0) the fluorescence response can be attributed to two different voltages. Both possible values are shown in Fig. 24 by solid and open circles respectively. The difference between alternative values can be as much as 1 V (Fig. 24) and is sensitive to small statistical errors.

With this ambiguity in mind it is important to notice that for every field strength the voltage is immediately exceeding 1 V at the anodic pole when an electric field is applied. For field strengths of 12.5 kV/cm and higher a subsequent further increase in transmembrane voltage is qualitatively consistent with simplified cell models, however, with charging time constants that are about six times longer than expected for an ideal insulating membrane. (70) For the lowest investigated field strength of 5 kV/cm, the data are strongly affected by the calibration ambiguity. Only for later times during the exposure can unambiguous values of about 1.1 V be assigned. This result suggests that voltage changes due to a contribution from charging currents are rather small compared to the initial dielectric effects which likely lead to the immediate jump in voltage to more than 1 V. Only eventually will the charging currents then shift the voltage towards slightly higher and unambiguous values.

After the initial sudden increase to 1 V the potential differences at the anodic pole continue to rise at a more moderate rate to ~1.6 V for applied field strengths equal to or greater than 50 kV/cm. Once this peak value is attained the transmembrane voltage begins to decrease and it is notable that this instant drop in voltage occurs *while* the electric field is still being applied. This event represents a threshold voltage has been reached. The rate of change from the initial jump up to the peak values is approximately the same for both hemispheres of the cell. However, the maximum transmembrane voltages at the anode lie between 1.4-1.6 V and between 0.5-0.6 V for the cathode pole. For all applied field strengths the cathode pole values are generally 1 V lower than the voltages at the anode side. For the lower field strengths of 5 kV/cm and 12.5 kV/cm voltages remain near the peak, once attained, throughout the remaining pulse duration and the distinct drop seen with application of higher field strengths is absent.

Once the electric field application is removed the resting transmembrane voltage starts to decrease again towards resting values. The ambiguities of the calibration for these smaller voltages do not allow us to determine the time constants of this decay exactly. Again the 5 kV/cm field strength effects are difficult to interpret since it appears that the voltage remains elevated long after the pulse application has ended. It is also worth mentioning that due to restrictions of our experimental setup an electric field with 20% the strength of the initial applied field remains for another 60 ns after the pulse. This may contribute to the residual elevated transmembrane voltages seen after the pulse.

Although the change in membrane potential was not expected to be biological in nature because of the ultra-fast timescale, verification that it was a sub-physiological response was tested by measuring the response of the cells to a 60 ns pulsed electric field of 90 kV/cm in the presence of several common ion channel blockers and also the use of a sodium-substituted buffer solution with glucamine. TEA, lanthanum, verapamil, nifedipine, diltiazem, TTX, and a sodium-substituted glucamine media were each evaluated separately for their effect on the response of the cells to nsPEF-induced changes in transmembrane potential. Only the use of TTX, a voltage-gated sodium channel blocker resulted in a transmembrane voltage change slightly higher than without (1.7 V instead of 1.6 V) but only at the anodic pole. The use of glucamine-substituted media decreased the degree of change of transmembrane voltage change at both the anode and cathode poles to 1.5 and 0.55 volts respectively (instead of 1.6 and 0.5 volts). All observed differences fall within an error range of three standard deviations and are therefore at least on this level not statistical significant. Thus we feel that the response in transmembrane potential is most likely sub-physiological.

DISCUSSION

A number of studies on the biological effects of nsPEF have suggested a dependency of the onset of cellular responses on the product of pulse duration and field strength. (21) On one hand a threshold can be defined by this convention which, when achieved, will induce a specific response of the cell such as apoptosis. (21) On the other hand, the primary physical processes, which are determined by the product of field strength and pulse duration, are electrical charging mechanisms. Consequently, a direct threshold effect in the transmembrane voltage of the plasma membrane is expected, which can be related to the observed biological responses. For very fast transients on the order of 1 ns dielectric effects will dominate the charging process as can be seen by the immediate rise of transmembrane voltages as soon as the electric field is applied. To study the charging of the cell membrane for different conditions we have developed a diagnostic

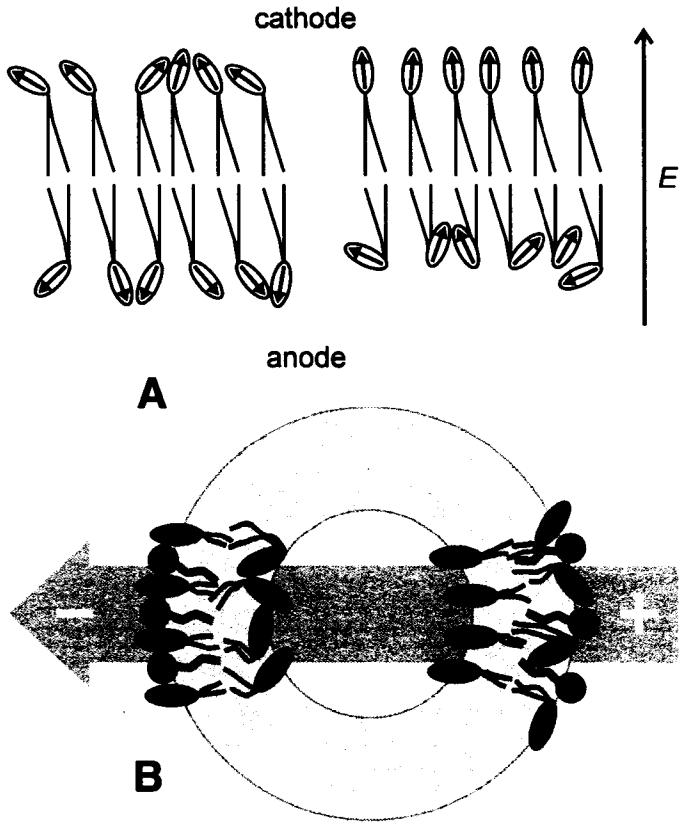

FIG. 25. **Dipole effect and transmembrane voltage asymmetry.** A) cartoon depicting neutral lipid molecules, which form the plasma membrane, under the influence of an applied electric field, B) transmembrane voltage asymmetry upon field application. Headgroup-dipoles of phospholipids are immediately aligned upon application of a strong electric field. This leads to a decrease of the local electric field strength at the location of dye-molecules in the outer leaflet at the cathode pole and to an increase at the anode pole respectively. This local field determines the fluorescence response.

method that allows measurements of transmembrane voltage changes in real-time, i.e. with a temporal resolution much shorter than the duration of the applied pulse. Our experiments support the hypothesis of a membrane charging threshold related to a biological response. To instigate a lasting physiological response it seems necessary to reach a transmembrane voltage of 1.4-1.6 V across the anodic hemisphere. Further development then likely depends on the possible formation of pores if the electric field is applied long after this threshold level is reached.

Remarkably the voltage across the cathodic pole is generally 1 V less than across the anodic pole. Two main mechanisms could contribute to this difference in transmembrane voltages: First, local perturbations in electric fields occur at the site of ANNINE-6 molecules embedded in the outer leaflet by the reorientation of lipid polar headgroups by the applied electric field. Without an electric field applied these headgroups are generally oriented (more or less) perpendicular to the membrane surface. Thermal motion though causes random deviations and fluctuations in the angle of the polarization vector as depicted in Fig. 25A. Since the quasi-negative charge of the headgroup dipole is closer to the lipid tail for almost all phospholipids, the polarization vector is generally pointing away from this tail when no electric field is applied. In a strong enough electric field, the dipoles will start to turn into the direction of this external field. The rotation occurs primarily at the outer anodic leaflet (and the inner leaflet at the cathode pole), though it is somewhat impeded by the torque imposed by the fatty acid tail anchor of the phospholipids (Fig.B). As a result of the dipole re-alignment, the local electric field will change, as the localized polarization (i.e., the screening ability) changes. This rapid dipole reorientation, which is expected to occur almost immediately, i.e. on a timescale of about 1 ns, when the electric field is applied, will change the local electric fields in the outer leaflet of the bilayer, *between* the headgroups of the phospholipids. At the anode pole the dipole screening weakens, whereas at the cathode pole the small and random changes in dipole orientation will not lead to a significant perturbation in the shielding of the applied electric field. Since the dye molecules of ANNINE-6 are embedded between the phospholipid headgroups of the outer leaflet their fluorescence response is determined by these local electric fields (externally applied less the dipole screening) as can be described by the molecular Stark effect. Notice that this dielectric effect, responsible for the voltage asymmetry between anode and cathode pole, does not require poration since the dipole swing is a fast "pre-poration" event that creates local "defects" which can eventually lead to a pore. Hence, it is understandable, due to this fast process, that the measured voltage change at the anode, in particular for exposures to 5 and 12.5 kV/cm, increases to more than 1 V almost instantaneously when an electric field is applied. In addition, since the reorientation of the headgroup dipoles will be the same, independent of their location on each hemisphere of the cell, an angular dependency of changes in fluorescence intensity is not expected. However, a distinct jump from one value to the other along the cell-equator (perpendicular to the applied electric field) is observed in our experiments (Fig. 23). Moreover the contributions of this dipole effect to the voltage difference across the membrane will last as long as an electric field of sufficient strength is applied.

Eventually charging mechanisms by ion currents will contribute more and more to the potential difference across the membrane and lead to a further increase in transmembrane voltage

above the values determined by this dipole effect. For a transmembrane voltage of more than 1 V the formation of pores is expected. According to the observed drop in voltage, after reaching peak voltages of 1.4-1.6 V, these mechanisms are ultimately responsible for the formation of pores in the membrane, which enable ion currents across this previously dielectric barrier and lead to a decrease in voltage even while the electric field is still applied. The creation of pores can also explain the asymmetrical charging *and* discharge response especially for the higher electric field strengths of 50 and 90 kV/cm. Several studies show that pores created at the cathode pole are in general larger. (84, 87, 103-105) In addition the lateral transport of negatively charged phosphatidylserine molecules towards or away from pores, depending at which pole the pores have formed, will either impede or promote the migration of ions through the pores. (106) The continuing increase in transmembrane potential up to values of 1.6 V at the anodic pole and 0.6 V at the cathodic side implies that during the rise to this value, the charging rate is greater than the ion exchange rate through the created pores. A suggested directionality for the transport of ions through a pore with respect to the direction of the applied electric field may furthermore contribute to the observed asymmetry in membrane potentials at opposite poles. (91)

The aforementioned ambiguities in the calibration of data for transmembrane voltages at the anode of 800 mV or less result in a difficult interpretation for measurements after the end of the 60 ns exposure when voltages continue to decrease. We consequently present both possible values of the transmembrane voltages at the anodic pole in Fig. 24 by open and solid circles respectively.

The development of the transmembrane voltages in particular at the anodic pole is strongly affected by the residual electric field after the first 60 ns of the exposure. During this post-exposure a field of still 20% the strength of the initially applied pulse is likely to sustain the orientation of headgroups for another 60 ns. Especially for the higher applied fields of 90 and 50 kV/cm the field during this second phase is comparable with the applied field of 5 kV/cm. This is sufficient to maintain a transmembrane voltage of about 1 V at the anodic pole although ion currents are already discharging the membrane. As soon as the field approaches zero, the orientation of the headgroups will become random accompanied by an almost sudden drop in transmembrane voltage. From this time on the measured values represent only the potential difference due to the remaining ion imbalance across the membrane. The loss of the orderly state of the dipole moments in the outer leaflet of the membrane at the anodic pole is determined by the energy threshold determined by the Brownian motion of the molecules. For lower field strengths of 5 and 12.5 kV/cm the energy provided by the reduced electric field in the post-exposure phase is falling below this threshold faster and accordingly we anticipate that the transmembrane voltage "jumps"

down to lower values earlier. Unfortunately our current set-up does not allow us to resolve this transition. It will require an improved pulse delivery system, which eliminates the residual electric field and to increase the dynamic response of the diagnostic for smaller transmembrane voltages for example by a different excitation.

As long as dipole-contributions to the local electric field in the membrane are high they mask the discharge of the membrane through conductive ion currents. When only a few or only small pores formed during the exposure, the membrane can only discharge slowly with a time constant identical to the charging time constant on the order of 100 ns. (8) This is the case for the lowest electric fields in our study. For exposure to 5 kV/cm the threshold value of 1.4-1.6 V that seems to indicate the onset of significant pore formation is not reached at all and for 12.5 kV/cm only towards the very end of the applied pulse. Accordingly the transmembrane voltage is not changing until the dipole orientation of lipid headgroups is lost up to 120 ns after the pulse at most. A faster conductive discharge after the pulse is however expected for higher electric fields when the threshold for membrane permeabilization is reached early during exposure, providing an additional discharge pathway. So far no direct experimental evidence for the proposed formation of small pores could be found. Traditional membrane integrity markers such as propidium iodide and ethidium homodimer are not permeable until several minutes after exposure (21, 64). The uptake is therefore considered a secondary response as these dyes pass through large pores that open later as a physiological response of the cell to the stimulation. From this experiment it is also apparent that the size of primary pores in the membrane, which are formed during the pulse and are responsible for conduction across the membrane, must be much smaller than the size of traditional membrane integrity molecules with a diameter suggested to be on the order of 1 nm (108).

Because the fastest biological response time is on the order of milliseconds the observed changes in transmembrane potential cannot be explained by a physiological response. This is confirmed by our control experiments with ion channel blockers. All measurements showed almost no effect of the blockers or substituted media on the membrane potential response to nsPEF. The measurements conducted during the exposure, however, do not exclude the possibility that physiological pathways will have been altered by the electric field. In fact, it is very likely that these pathways are significantly influenced by nsPEF stimulation (93) although an effect on membrane protein function is not expected to occur on a nanosecond timescale.

In closing, comparing the conditions that enable a cell to reach the threshold value for a sustained membrane poration to those reported to induce apoptosis suggest that the pulse parameters for electric field and pulse duration are similar (21). Within the range of electric fields that

are used in this study other work has shown that release of intracellular calcium, caspase activation, and phosphatidyl serine exposure can be attributed to nsPEF effects. (21, 69) We theorize that it is the initial plasma membrane or intracellular membrane effects on a nanosecond timescale that cause other signaling cascades (in the second to minute timescale) to be activated. The observed limits in transmembrane voltages, which are only slightly dependent on the field strength for higher electric fields, show that when the membrane is breached, subcellular structures are exposed to electric fields that are of similar magnitude to the applied electric field. Consequently, membrane effects similar to what we observe for the plasma membrane are expected and anticipated for intracellular membranes possibly interfering with cell signaling pathways (23, 69, 93). Further studies are necessary to substantiate this hypothesis derived from the limited number of data available for different exposure conditions. If this relationship can be established it will be possible to predict the conditions that are necessary to induce apoptosis. Based on this information treatments can be designed that aim for the selective removal of cells, in particular cancer cells.

CHAPTER V

CONCLUSIONS

The interaction of nanosecond pulsed electric fields with cells is not yet fully understood. From basic physical principles, we believe that charging mechanisms along membranes are the primary processes. In this respect, the interaction is similar to the mechanisms attributed to conventional electroporation pulses however the resulting pores that are formed are very different. With rise times on the order of 1 microsecond, ions can spread throughout the cell at the same rate as the increase of the electric field, so that the interior of the cell is almost instantaneously shielded from the applied electric field. Theses conventional electroporation pulses only charge the outer membrane and the pores that develop are larger and require longer times to reseal. Conversely, nanosecond pulses with rise times of only a few nanoseconds can penetrate the cell and interact with organelle-membranes, eventually leading to events that induce apoptosis. Due to their smaller size, organelles charge faster than the plasma membrane. With a pulse duration that is short compared to the charging time of the plasma membrane, nanosecond pulses have equal effect on internal membranes as they do on the plasma membrane. This behavior can readily be described with a rudimentary circuit model in which all membranes are ascribed the same electrical properties and are treated as ideal spherical capacitors (8, 70). It confirms that the threshold voltage required to create supra-electroporation, or pores much smaller and more numerous than those found with conventional electroporation, is reached for organelles before it is achieved across the outer membrane. The circuit model is based on various simplifications. Membrane dynamics and real organelle geometry are not taken into consideration. In fact, electrical properties and threshold voltages for organelle membranes are completely unknown thus far.

The analysis, within the framework of a simple circuit model, provides only a qualitative description of events. Modeling efforts, describing a cell and organelles as a whole, as well as molecular dynamics studies on the membrane level, are attempting to develop a more accurate understanding of the events during the application of a sub-microsecond pulse. Recent, theoretical, microdosimetry studies confirm the prediction that the effects of conventional electroporation pulses and nanosecond pulses are quite different (107). Both types of pulses eventually result in poration. However, conventional electroporation pulses have a significant effect only on the plasma membrane by inducing the formation of large pores. By contrast, pulses shorter than the charging time of the outer membrane of megavolt per meter field strength change the membrane potential of all membranes within the cell and induce much smaller pores or supra-

electroporation. With a charging time constant of 100 ns, the charging time for a cell with a 10 μm diameter is on the order of 300 ns. On the one hand, with electroporation pulses, the field is applied long enough so that pores with a diameter of sufficient size to allow the passage of molecules such as propidium iodide are formed. On the other hand, with ultra-short (nanoseconds) intense pulses (Megavolts per meter), pores are created more quickly than they can expand. As a result, the number of pores is several orders of magnitude higher than for electroporation pulses but the diameter of the pores is only about 0.8 nm. Accordingly, the effect of submicrosecond pulses is now described as "supra-electroporation" (107).

When the product of pulse duration and field strength reaches a certain threshold, a fast apoptotic cascade is initiated that leads to caspase activation in Jurkat cells within 30 minutes (21, 27). A similar response is also observed for HL-60 and HCT116 cells (8, 53, 108). In our opinion, the charging of subcellular membranes, which eventually leads to an increase in ion transfer across these structures, is one of the most likely mechanisms that trigger apoptotic cell death. The voltage across the membrane is a direct indicator of the accumulation of charge. Although the induction of apoptosis is already documented in several studies, no systematic correlation with the voltage across the membranes has yet been made. In the future, establishing the relationship between exposure parameters leading to apoptosis and the voltages across the plasma membrane and subcellular membranes is important. The data presented here indicate that, for Jurkat cells, a voltage of 1.6 V at the anodic pole of the membrane can be achieved, but only 0.6 V at the cathodic pole. Higher transmembrane voltages seem to be prevented by the flow of ions across the membrane. We don't yet know how long these conditions must be sustained to produce an apoptotic cell response. Moreover, in most studies on nanosecond-pulsed-electric-field-induced-apoptosis, multiple pulses were administered (3, 5, 10, or 100) with repetition rates of about 1 Hz. From our own experiments and recently published results by Vernier et al. (68, 101), we can already expect conformational changes of the membrane after the first pulse. If the membranes do not recover before the next pulse is applied, a cumulative effect is apparent. Consequently, studies on apoptotic thresholds of membrane potentials have to include, in addition to pulse duration and field strength, both the number of pulses and repetition rates. Therefore, future studies will need to expand greatly on the exposure parameters already defined in order to make correlations between changes in membrane potential to stimulation of signaling mechanisms including an apoptotic cascade. Since induced ion currents across cellular membranes will interfere strongly with established signaling pathways we think this scenario is responsible for the induction of apoptosis.

REFERENCES

1. Schoenbach, K. H., Katsuki, S., Stark, R. H., Buescher, E. S., and Beebe, S. J (2002) *IEEE Trans. Plasma Sci.* **30**, 293-300
2. Gowrishankar, T. R., and Weaver, J. C. (2003) Proc Natl Acad Sci USA. **100**, 3203-3208
3. Weaver, J. C. (1994) *Ann NY Acad Sci.* **720**, 141-152
4. Weaver, J. C. (2000) *IEEE Trans. Plasma Sci.* **28**, 24-33
5. Gehl, J. (2003) *Acta Physiol Scand.* **177**, 437-447
6. Teissie, J. (1994) *Ann NY Acad Sci.* **720**, 98-110
7. Cole, K. S. (1937) *Trans. Faraday Soc.* **33**, 966-972
8. Schoenbach, K. H., Beebe, S. J., and Buescher, E. S. (2001) *Bioelectromagnetics* **22**, 440–448
9. Neumann, E., Schaefer-Ridder, M., Wang, Y., and Hofschneider, P. H. (1982) *EMBO J.* **1**, 841-845
10. Weaver, J. C. (1993) *J. Cell Biochem.* **51**, 426-435
11. Heller, R., Jaroszeski, M. J., Glass, L. F., Messina, J. L., Rapaport, D. P., Deconti, R. C., Fenske, N. A., Gilbert, R. A., Mir, L. M., and Reintgen, D. S. (1996) *Cancer* **77**, 964-971
12. Mir, L. M., (1999) Proc Natl Acad Sci USA. **96**, 4262-4267
13. Tsong, T. (1991) *Biophys. J.* **60**, 297-306
14. Neumann, E., Kakorin, S., and Toensing, K. (1999) *Bioelectrochem Bioenerg.* **48**, 3-16
15. Golzio, M. (1998) *Biophys J.* **74**, 3015-3022
16. Prausnitz, M. R., Corbitt J. D., Gimm J. A., Golan, D. E., Langer, R., and Weaver, J. C. (1995) *Biophys J.* **68**, 1864-1870
17. Djuzenova C. S. (1996) *Biochim Biophys Acta.* **1284**, 143-152
18. Lee, M. J. (2002) *Exp Mol Med.* **34**, 265-272

19. Müller, K. J., Sukhorukov, V. L., and Zimmermann, U. (2001) *J Membr Biol.* **184**, 161-170

20. Schoenbach, K. H., Peterkin, F. E., Alden, R. W., III, and Beebe, S. J. (1997) *IEEE Trans Plasma Sci.* **25**, 284-292

21. Beebe, S. J., Fox, P. M., Rec, L. J., Willis, L. K., and Schoenbach, K. H. (2003) *FASEB J.* **17**, 1493-1495

22. Beebe, S. J., White J., Blackmore, P. F., Deng, Y., Sommers, D., and Schoenbach, K. H. (2003) *DNA Cell Biol.* **22**, 785-796

23. Vernier, P. T., Sun, Y., Marcu, L., Salemi, S., Craft, C. M., and Gundersen, M. A. (2003) *Biochem Biophys Res Commun.* **310**, 286-295

24. Yuan, J., and Li, H. (1999) *Curr Opin Cell Biol.* **11**, 261-266

25. Adams J. M. (2003) *Genes and Dev.* **17**, 2481-2495

26. Hair, P. S., Schoenbach, K. H., and Buescher, E. S. (2003) *Bioelectrochemistry.* **61**, 65-72

27. Beebe, S. J., Fox, P. M., Rec, L. J., Somers, K., Stark, R. H., and Schoenbach, K. H. (2002) *IEEE Trans. Plasma Sci.* **30**, 286–292

28. Nuccitelli R., Pliquett, U., Chen X., Ford, W., James Swanson, R., Beebe, S. J., Kolb, J. F., and Schoenbach, K. H. (2006) *Biochem Biophys Res Commun.* **343,** 351-360

29. Berridge, M. J. (2003) *Nat. Rev. Mol. Biol.* **4**, 517–529

30. Berridge, M. J., Bootman, M. D., and Lipp, P. (1998) *Nature*. **395**, 645-648

31. Weaver, J. C. (2000) in *Biomedical Engineering Handbook* (Bronzino, J. D., ed) pp. 1431–1440, CRC Press, Inc., and IEEE Press, Boca Raton, FL

32. Weaver, J. C., and Chizmadzhev, Y. (1996) in *CRC Handbook of Biological Effects of Electromagnetic Fields* (Polk, C., and Postow, E., eds) 2nd Ed., pp. 247–274, CRC Press Inc., Boca Raton, FL

33. Zimmerman, U., Friedrich, U., Mussauer, H., Gessner, P., Hamel, K., and Sukhorukov, V. (2000) *IEEE Trans. Plasma Sci.* **28**, 72–82

34. Dev, S. B., Rabussay, D. A., Widera, G., and Hofmann, G. A. (2000) *IEEE Trans. Plasma Sci.* **28**, 206–223

35. Chang, D. C. (1992) in *Guide to Electroporation and Electrofusion* (Chang, D. C., Chassy, B. M., Saunders, J. A., and Sowers, A. E., eds) pp. 1–6, Academic Press, Orlando, FL

36. Neumann, E., Schafer-Ridder, M., Wang, Y., and Hofschneider, P. H. (1982) *EMBO J.* **1**, 841-845

37. Wong, T. K., and Neumann, E. (1982) *Biochem. Biophys. Res. Commun.* **107**, 584–587

38. Weaver, J. C., Vaughan, T. E., and Chizmadzhev, Y. (1999) *Adv. Drug Delivery Rev.* **35**, 21–39

39. Belehradek, M., Domenge, C., Luboinski, B., Orlowski, S., Belehradek, J., Jr., and Mir, L. M. (1993) *Cancer (Phila.)* **72**, 3694–3700

40. Dev, S. B., and Hofmann, G. A. (1994) *Cancer Treat. Rev.* **20**, 105–115

41. Alemany, R., Sichelschmidt, B., zu Heringdorf, D. M., Lass, H., van Koppen, C. J., and Jakobs, K. H. (2000) *Mol. Pharmacol.* **58**, 491–497

42. Verghese, M. W., Kneisler, T. B., and Boucheron, J. A. (1996) *J. Biol. Chem.* **271**, 15597–15601

43. Klinker, J. F., Wenzel-Seifert, K., and Seifert, R. (1996) *Gen. Pharmacol.* **27**, 33–54

44. Lee, H., Suh, B. C., and Kim, K. T. (1997) *J. Biol. Chem.* **272**, 21831–21838

45. Suh, B. C., Kim, T. D., Lee, I. S., and Kim, K. T. (2000) *Br. J. Pharmacol.* **131**, 489–497

46. Nilius, B. (2003) *Cell Calcium.* **33**, 293–298

47. Heiner, I., Eisfeld, J., Halaszovich, C. R., Wehage, E., Jungling, E., Zitt, C., and Luckhoff, A. (2003) *Biochem. J.* **371**, 1045–1053

48. Heiner, I., Eisfeld, J., and Luckhoff, A. (2003) *Cell Calcium* **33**, 533–540

49. Itagaki, K., and Hauser, C. J. (2003) *J. Biol. Chem.* **278**, 27540–27547

50. Venkatachalam, K., van Rossum, D. B., Patterson, R. L., Ma, H. T., and Gill, D. L. (2002) *Nat. Cell Biol.* **4**, E263–E272

51. Buescher, E. S., and Schoenbach, K. H. (2003) *IEEE Trans. on Dielectrics and Electr. Insul.* **10**, 788–794

52. Bobanovic, F., Bootman, M. D., Berridge, M. J., Parkinson, N. A., and Lipp, P. (1999) *FASEB J.* **13**, 365–376

53. Deng, J., Schoenbach, K. H., Buescher, E. S., Hair, P. S., Fox, P. M., and Beebe, S. J. (2003) *Biophys. J.* **84**, 2709–2714

54. Dobrydneva, Y., and Blackmore, P. (2001) *Mol. Pharmacol.* **60**, 541–552

55. Grinstein, S., and Furuya, W. (1988) *J. Biol. Chem.* **263**, 1779–1783

56. Gallois, A., Bueb, J. L., and Tschirhart, E. (1998) *Eur. J. Pharmacol.* **361**, 293–298

57. Treiman, M., Caspersen, C., and Christensen, S. B. (1998) *Trends Pharmacol. Sci.* **19**, 131–135

58. Harper, J. L., Camerini-Otero, C. S., Li, A. H., Kim, S. A., Jacobson, K. A., and Daly, J. W. (2003) *Biochem. Pharmacol.* **65**, 329–338

59. Hamilton, W. A., and Sale, A. J. H. (1967) *Biochim. Biophys. Acta.* **148**, 789–800

60. Weaver, J. C., and Chizmadzhev, Y. A. (1996) *Bioelectrochem. Bioenerg.* **4**, 135–160

61. Hofmann, G. A., Dev, S. B., Nanda, G. S., and Rabussay, D. (1999) *Crit. Rev. Ther. Drug Carrier Syst.* **16**, 523–569

62. Widera, G., Austin, M., Rabussay, D., Goldbeck, C., Barnett, S. W., Chen, M. C., Leung, L., Otten, G. R., Thudium, K., Selby, M. J., and Ulmer, J. B. (2000) *J. Immunol.* **164**, 4635–4640

63. Lucas, M. L., and Heller, R. (2003) *DNA Cell Biol.* **22**, 755–763

64. Chen, N., Schoenbach, K. H., Kolb, J. F., James, S. R., Garner, A. L., Yang, J., Joshi, R. P., and Beebe, S. J. (2004) *Biochem. Biophys. Res. Commun.* **317**, 421–427

65. Hu, Q., Viswanadham, S., Joshi, R. P., Schoenbach, K. H., Beebe, S. J., and Blackmore, P. F. (2005) *Phys. Rev. E. Stat. Nonlin. Soft. Matter Phys.* **71**, 031914-1-031914-9

66. Schultheiss, C., Bluhm, H., Mayer, H. G., Kern, M., Michelberger, T., and Witte, G. (2002) *IEEE Transactions on Plasma Science.* **30**, 1547–1551

67. Schoenbach, K. H., Joshi, R. P., Stark, R. H., Dobbs, F. C., and Beebe, S. J. (2000) *IEEE Transactions on Dielectrics and Electrical Insulation.* **7**, 637–645

68. Vernier, P. T., Sun, Y. H., Marcu, L., Craft, C. M., and Gundersen, M. A. (2004) *FEBS Lett.* **572**, 103–108

69. White J. A., Blackmore, P. F., Schoenbach, K. H., and Beebe, S. J. (2004) *J Biol Chem.* **279**, 22964-22972

70. Schoenbach, K. H., Joshi, R. P., Kolb, J. F., Chen, N. Y., Stacey, M., Blackmore, P. F., Buescher, E. S., and Beebe, S. J. (2004) *Proc. IEEE.* **92**, 1122–1137

71. Kinosita, K., Jr., Ashikawa, I., Saita, N., Yoshimura, H., Itoh, H., Nagayama, K., and Ikegami, A. (1988) *Biophys. J.* **53**, 1015–1019

72. Hubener, G., Lambacher, A., and Fromherz, P. (2003) *J. Phys. Chem. B.* **107**, 7896–7902

73. Kuhn, B., and Fromherz, P. (2003) *J. Phys. Chem. B.* **107**, 7903–7913

74. Loew, L. M., Bonneville, G. W., and Surow, J. (1978) *Biochemistry.* **17**, 4065–4071

75. Loomis-Husselbee, J. W., Cullen, P. J., Irvine, R. F., and Dawson, A. P. (1991) *Biochem. J.* **277**, 883–885

76. Tomov, T., and Tsoneva, I. (2000) *Biochemistry.* **51**, 207–209

77. Kolb, J. F., Kono, S., and Schoenbach, K. H. (2005) *Bioelectromagnetics.* **27**, 172–187

78. Xu, C., Zipfel, W., Shear, J. B., Williams, R. M., and Webb, W. W. (1996) *Proc. Natl. Acad. Sci. USA.* **93**, 10763–10768

79. Kuhn, B., Fromherz, P., and Denk, W. (2004) *Biophys. J.* **87**, 631–639

80. Sarkadi, B., Tordai, A., and Gardos, G. (1990) *Biochim. Biophys. Acta.* **1027**, 130–140

81. Fischer, J. K., von Bruning, D. M., and Labhart, H. (1976) *Appl. Opt.* **15**, 2812–2816

82. Stewart, D. A., Gowrishankar, T. R., and Weaver, J. C. (2004) *IEEE Transactions on Plasma Science.* **30**, 1696–1708

83. Loew, L. M. (1999) *In* Fluorescent and Luminescent Probes for Biological Activity. E. Mason, editor. Academic Press. New York. 210–221

84. Tekle, E., Astumian, R. D., and Chock, P. B. (1990) *Biochem. Biophys. Res. Commun.* **172**, 282–287

85. Mehrle, W., Hampp, R., and Zimmermann, U. (1989) *Biochim. Biophys. Acta.* **978**, 267–275

86. Tekle, E., Astumian, R. D., and Chock, P. B. (1994) Selective and asymmetric molecular transport across electroporated cell membranes. *Proc. Natl. Acad. Sci. USA.* **91**, 11512–11516

87. Tekle, E., Astumian, R. D., Friauf, W. A., and Chock, P. B. (2001) *Biophys. J.* **81**, 960–968

88. Siwy, Z., and Fulinski, A. (2004) *Am. J. Phys.* **72**, 567–574

89. Siwy, Z., and Fulinski, A. (2002) *Phys. Rev. Lett.* **89**, 198103–1-198103–4

90. Astumian, R. D. (1997) *Science.* **276**, 917–922

91. Hu, Q., Sridhara, V., Joshi, R. P., Kolb, J. F., Schoenbach, K. H. (2006) *IEEE Trans. Plasma Sci.* **34**, 1405-1411

92. Haest, C. W. M., Kamp, D., and Deuticke, B. (1997) *Biochim. Biophys. Acta.* **1325**, 17–33

93. Beebe, S. J., and Schoenbach, K. H. (2005) *J Biomed Biotechnol.* **4**, 297-300

94. Teissie, J., Eynard, N., Vernhes, M. C., Benichou, A., Ganeva, V., Galutzov, B., and Cabanes, P. A. (2002) *Bioelectrochemistry.* **55**, 107-112

95. Joshi, R. P., Hu, Q., and Schoenbach, K. H. (2004) *IEEE Trans. Plas Sci.* **32**, 1677-1688

96. Krassowska, W., and Neu, J. C. (1994) *Biohpys J.* **66**, 1768-1776

97. Knisley, S. B., Blitchington, T. F., Hill, B. C., Grant, A. O., Smith, W. M., Pilkington, T. C., and Ideker. R. E. (1993) *Circ Res.* **72**, 255-270

98. Simcic, S., Bobanovic, F., Kotnik, V., and Vodovnik, L. (1997) *Phsiol Chem Phys Med NMR.* **29**, 39-50

99. Teissie, J., Golzio, M., and Rols, M. P. (2005) *Biochim Biophys Acta.* **1724**, 270-280

100. Beebe, S. J., Blackmore, P. F., White, J., Joshi, R. P., and Schoenbach, K. H. (2004) *Physiol Meas.* **25**, 1077-109

101. Vernier, P. T., Sun, Y., Marcu, L., Craft, C. M., and Gunderson, M. A. (2004) *Biophys J.* **86**, 4040-4048

102. Frey, W., White, J. A., Price, R. O., Blackmore, P. F., Joshi, R. P., Nuccitelli, R. L., Beebe, S.J., Schoenbach, K.H., and Kolb, J.F. (2006) *Biophys J.* **90**, 3608-3615

103. Lojewska, R. P., Farkas, D. L., Ehrenberg, B., and Loew, L. M. (1989) *Biophys J.* **56**, 121-128

104. Tarek, M. (2004) *Biophys J.* **88**, 4045-4053

105. Leontiadou, H., Mark, A. E., and Marrink, S. J. (2004) *Biophys J.* **86**, 2156-2164

106. Hu Q., Joshi, R. P., and Schoenbach, K. H. (2005) *Phys Rev E.* **72**, 031902-1-031902-10

107. Gowrishankar, T. R., Esser, A. T., Vasilkoski, Z., Smith, K. C., and Weaver, J. C. (2006) *Biochem. Biophys. Res. Commun.* **341**, 1266–1276

108. Hall, E. H., Schoenbach, K. H., and Beebe S. J. (2005) *DNA Cell Bio.l* **24**, 283-291

APPENDIX

COPYRIGHT PERMISSIONS

Copyright Permission Policy

ASBMB Journals
Journal of Biological Chemistry
Molecular and Cellular Proteomics
Journal of Lipid Research
Biochemistry and Molecular Biology Education
ASBMB Today

ASBMB does not charge for and grants use without requiring your copyright permission request for:

- Original authors wanting to reproduce portions of their own work; or to republish their material in not-for-profit formats or venues.
- Students wanting to reproduce or republish their work for educational purposes.
- Students using other authors' material for their theses.
- Reproduction or republication of abstracts only.
- Photocopying up to 5 copies for personal use.
- Non-profit educational institutions making multiple photocopies of articles for classroom use all such reproduction must utilize institutionally owned equipment for this purpose.

Use of copyrighted material requires proper citation.

Biophysical Society

Biophysical Journal
Copyright Permission Form

In order to obtain copyright permission, please answer the questions below. When you have completed the form you may fax it to (301) 634-7267 or email it as an attachment to bi@biophysics.org. Once your request is processed, it will be sent back to you for your records.

Name: Jody A. White

Address: 618 Raleigh Ave. Apt #1
NORFOLK, VA 23507

Phone: 757 - 450 - 0700

Fax: 757 - 314 - 2397

Email: jaws28403@yahoo.com

★ - please fax permission if possible! ☺

I am requesting permission to reprint Figure(s) 1 - 8 (figure numbers) by Frey, White, Price, Blackman, Joshi, Vasilkoski, Beebe, Schwerbach, Kolb (author names) from the article Plasma Membrane Voltage Changes during Nanosecond Pulsed Electric Field Exposure (title) in Biophys. J. 2006 (year) 90 (vol.) 3608-15 (issue) (page numbers). I understand that I am obligated to notify the original author(s) and will provide appropriate attribution to the Biophysical Society and said author(s) for use of these materials.

OFFICE USE ONLY:

Permission granted Alisha Yocum Date 11/7/06

VITA

JODY ANNE WHITE

Frank Reidy Research
Center for Bioelectrics,
Old Dominion University
830 Southampton Avenue, Suite 5100,
Norfolk, Virginia 23510

Eastern Virginia Medical School
825 Fairfax Ave.
Norfolk, Virginia 23501

Education:

B.S., University of North Carolina at Wilmington, Biology, 1998

Ph.D., Old Dominion University, Biochemistry, Norfolk, VA 2006

Professional Experience:

Center for Bioelectrics, Graduate Research Assistant Appointed: 2002

2001-2002, Teaching Assistant, Old Dominion University, Chemistry

2000-2001, Teaching Assistant, North Carolina State University

1998-1999, Assistant Scientist I, Applied Analytical Industries

Publications:

- Frey W, White JA, Price RO, Blackmore PF, Joshi RP, Nuccitelli RL, Beebe SJ, Schoenbach KH, Kolb JF, Plasma Membrane Voltage Changes During Nanosecond Pulsed Electric Field, *Biophysical Journal*, **90**(10):3608-15, May 2006.
- Beebe SJ, Blackmore PF, White J, Joshi RP, Schoenbach KH, Nanosecond pulsed electric fields modulate cell function through intracellular signal transduction, *Physiological Measurement*, **25**(4):1077-93, August 2004.
- White JA, Blackmore PF, Schoenbach KH, Beebe SJ, Stimulation of capacitative calcium entry in HL-60 cells by nanosecond pulsed electric fields (nsPEFs), *Journal of Biological Chemistry*, **279**(22):22964-72, May 2004.
- Beebe SJ, White J, Blackmore PF, Deng Y, Somers K, Schoenbach KH, Diverse Effects of Nanosecond Pulsed Electric Fields on Cells and Tissues, *DNA and Cell Biology* (Annual Review), **22**(12):785-96, December 2003.